

# The distributional benefits of emission reductions from renewable energy

Daniel T. Kaffine\* Nicole J. Mundt†

March 21, 2023

## Abstract

Renewable electricity generation has dramatically expanded in the last decade, with important consequences for local emissions reductions and air quality. In this paper, we estimate the distributional benefits from reductions in local emissions due to utility-scale wind and solar generation using hourly data from California electricity markets. We find that while the reductions in fossil generation and emissions at the plant-level are roughly evenly split across poverty rates and racial composition, there is a substantial disparity between high and low population areas - generation and emissions from rural power plants are an order of magnitude more responsive to renewables compared to more urban power plants. Pollution transport modeling confirms pollution reductions are largest in rural areas and finds additional benefits for areas with a greater share of non-white households. We show transmission and proximity to renewable capacity play key roles in determining the pattern of fossil fuel plant responses.

JEL Codes:

Keywords: Wind power, solar power, environmental justice, distributional effects, transmission

---

\*Kaffine: Department of Economics, University of Colorado Boulder, 256 UCB Boulder CO, 80309 USA, daniel.kaffine@colorado.edu.

†Mundt: Department of Market Monitoring, California Independent System Operator. 250 Outcropping Way Folsom CA, 95630 USA, nicole.mundt@colorado.edu. \*\*This paper is based solely on publicly available data and is not necessarily representative of the Department of Market Monitoring's views.

# 1 Introduction

The remarkable worldwide growth of renewable electricity generation in the last decade has brought about a substantial transformation of electricity markets and the grid, offsetting fossil fuel-based electricity generation and reducing global and local emissions. In 2020, more than 400 million megawatt-hours (MWh) of wind and solar electricity were produced in the United States, leading to local environmental benefits on the order of tens of billions of dollars; however, less is known about the distribution of those local air quality benefits. This is particularly surprising given emerging concerns regarding air quality, the electricity sector, and environmental justice (EJ), which nearly derailed the renewal of the carbon cap and trade program in California. Such market-oriented policies have been oft-criticized from an environmental justice standpoint, while policies to promote renewable energy have been proposed as a more environmentally just approach to environmental and climate policy. As such, we ask: what are the demographics of the households who have benefited from the renewable-induced emissions reductions from fossil fuel generation, and what are the mechanisms that drive different distributional outcomes?

In this paper, we exploit exogenous hourly variation in renewable energy generation to recover causal estimates of generation and emissions responses by fossil fuel generators to utility-scale wind and solar generation. We link these fossil fuel plants and their generation and emissions responses to the socioeconomic characteristics of the population near the power plant. This allows us to decompose the overall reduction in fossil generation and emissions across different demographic cuts of the local population, such as racial composition, poverty rates, and population, considering impacts in terms of plant location and also pol-

lution dispersal. In order to inform policymaking related to power plant retirement, siting, and transmission decisions, we then analyze the mechanisms underlying these distributional outcomes as well as the profit implications for fossil fuel generators.

Our analysis has several key features. First, we obtain socioeconomic characteristics near fossil fuel plants (3 kilometers in our central specification) in order to identify which types of households are benefiting from reductions in local emissions. Second, we leverage approximately two years of rich hourly generation and emissions data from California to exploit plausibly exogenous variation in wind and solar generation to recover causal estimates. California is a particularly compelling location to study the distributional effects of renewables, given the large share of both wind and solar energy in the state, the concerns noted above regarding environmental justice and the electricity sector, and the state’s ambitious renewable goals of 100% by 2045.<sup>1</sup> Third, we explore heterogeneity in these causally-estimated responses of fossil fuel plants to renewables, comparing responses across poverty share, racial composition, and population levels. The plant-level emission responses are also run through a pollution-transport model (InMap) to understand the patterns of pollution dispersal in terms of community demographics. Finally, while related studies on the EJ properties of environmental markets (discussed further below) are often data-constrained to plant-level annual emissions, our hourly generation and emissions data allows for a richer exploration of mechanisms, including tying hourly generation and emission responses to hourly local marginal prices and congestion costs for electricity. While two recent, related papers es-

---

<sup>1</sup> Several environmental justice groups strongly opposed the extension of California’s carbon cap and trade program, as noted here: <https://www.npr.org/2017/02/24/515379885/environmental-groups-say-californias-climate-program-has-not-helped-them>. The final rulemaking summary by the California Air Resource Board contains many references to “Environmental Justice” throughout, and how the agency responded to the concerns raised: <https://ww3.arb.ca.gov/regact/2018/capandtrade18/ct18fsor.pdf>.

estimate the nationwide distributional impacts of wind (Qiu et al. 2022) and rooftop solar (Harris and Dauwalter 2022), our focus on the electricity sector mechanisms that give rise to the distributional outcomes is distinct.

A priori, the distribution of emission benefits from renewables is not obvious, as several mechanisms may be at play. On the one hand, a *merit order effect* might be critical if older, dirtier, more costly, or less efficient plants are more likely to be pushed off the margin by renewables, reducing their generation and emissions (Fell and Kaffine 2018; Callaway et al. 2018). To the extent these older, dirtier plants are located near disadvantaged groups, air quality improvements from renewables may disproportionately accrue to those groups. On the other hand, a *transmission effect* might be more important if location and transmission constraints plays a more dominant role (Davis and Hausman 2016; Fell et al. 2021; Gonzales et al. 2022). If transmission capacity constraints spatially affect the set of responding fossil fuel generators, then communities located near wind and solar generators may disproportionately benefit. In California, these wind and solar generators are concentrated in the central and eastern part of the state, while most of the main population centers are along the western coast (see Appendix Figure A.1).

We find fossil generation and emissions reductions are split roughly equally across poverty rates and racial/ethnic groups in California - fossil fuel plants in the top and bottom terciles of poverty rates and racial/ethnic composition respond to renewables to approximately the same degree. However, we find an order-of-magnitude larger reduction in fossil generation and emissions in the bottom tercile of population compared to the top tercile; rural areas of California see much larger reductions in local emissions compared to the denser coastal areas. Using pollution transport modeling to capture pollution dispersion, we find again

that the largest ground-level PM 2.5 reductions occur in rural areas, but in contrast to the plant-level results, we do find some evidence that areas with a greater share of non-white households have benefitted more.

Additional analysis supports the *transmission effect* as the primary mechanism for the large rural response. For example, natural gas plants with the largest nearby renewable capacity tend to be located in more rural areas, and a natural gas plant with an additional 1000 megawatts (MW) of renewable capacity nearby has a 40% larger response to renewable generation. Furthermore, we show these fossil fuel plants in lower population areas also see greater reductions in hourly electricity prices (due to transmission congestion) in response to increases in wind and solar generation. By contrast, heat rates and fuel costs, essential features of the *merit order effect* through their impact on the marginal cost of generation, play a much more limited role in explaining the large emission reductions in rural areas. Finally, using our estimates of quantity and price responses to renewables, we show that an additional 1000 MWh of solar results in a negative congestion effect on natural gas plant profitability in low population areas that is 2.5 larger compared to higher population areas.

Our findings have several important implications. First, a growing body of literature highlights the importance of air pollution for health outcomes (Currie and Walker 2011; Schlenker and Walker 2016; Deschênes et al. 2017; Deryugina et al. 2019; Rivera et al. 2021), and our analysis provides insight into how the local health benefits of renewables are distributed. Second, environmental justice has emerged as an important consideration in policymaking, with environmental justice concerns related to environmental markets in California receiving substantial attention in the academic literature (Fowlie et al. 2012; Cushing et al. 2018; Grainger and Ruangmas 2018; Lukanov and Krieger 2019; Hernandez-

Cortes and Meng 2023; Shapiro and Walker 2021; Mansur and Sheriff 2021).<sup>2</sup> Third, substantial investments have been made in renewables in the last decade, particularly utility-scale wind and solar, including more than \$55 billion in 2019 in the United States and nearly \$300 billion worldwide.<sup>3</sup> These investments are justified in part by cleaning up local air quality (Bento et al. 2018), and our analysis provides insights into the recipients of those air quality benefits.

Finally, our findings are important for a number of active policy debates. First, as part of their 20-year transmission outlook plan, the California ISO, California Energy Commission, and California Public Utilities Commission identified 15 GW of natural gas capacity to be retired by 2040, with a priority on the oldest natural gas plants located within a 2.5-mile radius of disadvantaged communities.<sup>4</sup> Most of these natural gas plants are in the Bay Area and LA Basin area, and we find their profitability is reduced by utility-scale renewables much less than rural plants. Even if renewables continue to grow in share, proximity to renewable capacity is likely to drive retirements, while proximity to disadvantaged communities is not. Second, and more generally, we show that transmission is an important determinant of the distribution of emission reductions, and thus there is an overlooked environmental justice

---

<sup>2</sup> An important consideration that has emerged in this literature is the modeling of pollution dispersion across space and potentially different demographic groups). Given our interest in understanding the supply-side mechanisms, we follow Fowlie et al. (2012), Shapiro and Walker (2021), and others in focusing our analysis and discussion on demographics near fossil fuel plants (a radius-based approach), complementing these findings with reduced-complexity pollution transport modeling via InMap Tessum et al. (2017). An alternative approach would be to model the pollution dispersion using more sophisticated atmospheric dispersion models such as HYSPLIT (Grainger and Ruangmas 2018; Hernandez-Cortes and Meng 2023) or GEOS-Chem Qiu et al. (2022), which can produce more detailed pollution distribution profiles based on meteorological conditions. InMap is commonly used for policy analysis and is a reasonable compromise of complexity and computational speed given our focus and contribution on the mechanisms behind the distribution of emission reductions as mediated by transmission and electricity markets.

<sup>3</sup> Per a recent Bloomberg Report: <https://about.bnef.com/clean-energy-investment/>.

<sup>4</sup> See <http://www.caiso.com/InitiativeDocuments/20-YearTransmissionOutlook-May2022.pdf>, page 20 “Table 3.1-4: Assumed gas-fired generation retired by local capacity area”

component of transmission planning. While we find that rural Californians have primarily benefited from reduced emissions from utility-scale renewables, this distribution of benefits can be altered with transmission investment, if desired by policymakers. Relatedly, given that the majority of US states have adopted renewable portfolio standards (RPS) and there is a current push for a federal renewable electricity standard, our findings also provide guidance on the EJ implications of adopting or expanding these renewable policies.<sup>5</sup> For example, Qiu et al. (2022) show that 29% of RPS benefits accrued to racial/ethnic minorities and 32% of RPS benefits accrued to low-income groups, both of which are below the target of 40% set by the Biden Administration. Our findings suggest transmission infrastructure may be an important lever for meeting those EJ targets.

This paper contributes to several literatures, including the recent literature on the environmental consequences of renewable electricity, which estimates the emission savings from wind (Cullen 2013; Kaffine et al. 2013; Novan 2015; Callaway et al. 2018; Fell and Kaffine 2018), with a smaller but growing literature on solar emission savings (Baker et al. 2013; Millstein et al. 2017; Sexton et al. 2021). This paper also relates to the literature showing that spatial heterogeneity in the electricity sector is important and that location matters for the environmental value of renewables (Muller and Mendelsohn 2009; Zivin et al. 2014; Holland et al. 2016; Fell et al. 2021). Finally, this paper also contributes to the broader literature on air quality, energy systems, and environmental justice (Li et al. 2019; Bento et al. 2015; Mueller and Brooks 2020; Chapman et al. 2018; Borenstein and Davis 2016;

---

<sup>5</sup> For example, a recent letter from 715 organizations strongly encouraged Congress to enact a federal renewable electricity standard: [https://www.biologicaldiversity.org/programs/energy-justice/pdfs/2021-5-12\\_600-Group-Letter-for-RES.pdf](https://www.biologicaldiversity.org/programs/energy-justice/pdfs/2021-5-12_600-Group-Letter-for-RES.pdf). While there has been discussion regarding what sorts of technologies should “count” as clean or renewable, the core commitment to renewable electricity standards as an environmentally just approach appears to enjoy broad support across many environmental groups.

Holland et al. 2019), as well as environmental justice concerns more broadly (Banzhaf et al. 2019; Currie et al. 2020). Along with Qiu et al. (2022) and Harris and Dauwalter (2022), we causally identify the distributional consequences of emission reductions from renewable energy, and to our knowledge, our analysis is the first to empirically identify the importance of transmission mechanisms for understanding those distributional consequences.

## 2 Methods

### 2.1 Data

In order to establish who benefits from emissions reductions via increased renewable generation, we need to determine which fossil fuel generators are reducing their generation and emissions in response to solar and wind generation. With the largest amount of solar generation in particular, data from the California Independent System Operator (CAISO) provide useful variation for estimating wind and solar emission savings. We first describe the hourly electricity data used to estimate the fossil generation and emissions response to solar and wind generation. We then describe the demographic data used to determine the population within 3 miles of each fossil generator that may be reducing its generation (and emissions) in response to increased renewable generation.

#### 2.1.1 Electricity data

Our sample starts in April 2018, due to the availability of hourly solar generation from the California Independent Systems Operator (CAISO), and goes through December 2019. It consists of hourly data such as fuel mix and imports. Hourly load data across the four

utility regions in CAISO is available through the Energy Information Administration (EIA). These four regions include Pacific Gas and Electric (PG&E), Southern California Edison (SCE), San Diego Gas and Electric (SD&E), and Valley Electric Association (VEA). Hourly imports and generation by fuel type are obtained through CAISO. We also include hourly temperature data from the National Oceanic and Atmospheric Administration (NOAA) and daily Henry Hub price provided by the EIA. We supplement with hourly data on natural gas generators provided by the Environmental Protection Agency’s (EPA) Continuous Emissions Monitoring (CEMS) database. These generator-level characteristics include hourly generation, fuel input, and emission rates of nitrogen oxides ( $\text{NO}_x$ ). While we do not have direct measurements for hourly emissions of other local pollutants such as particulate matter (PM<sub>2.5</sub>), carbon monoxide (CO) and volatile organic compounds (VOC), hourly generation responses will proxy for the emission response to renewables for non- $\text{NO}_x$  local pollutants. Per Table 1, during this period solar and wind generation account for an average of 12.6% and 7.6% of hourly load in CAISO, respectively.

### **2.1.2 Demographic data**

Demographic data on the population within 3 miles of the plants in California is available through the Physicians, Scientists, and Engineers for Healthy Energy (PSE) organization. PSE matches each plant to its census bloc, which allows incorporation of data from the U.S. Census Bureau, the American Community Survey (ACS), and the CalEnviroScreen 3.0.<sup>6</sup> Together these sources provide data on the number of individuals living within 3 miles of each natural gas plant, the median income of those individuals, the percent living below the

---

<sup>6</sup> More information on the methods used by PSE to match generators to demographic data can be found here: <https://www.psehealthyenergy.org/wp-content/uploads/2018/11/California-Power-Map-Methods.pdf>.

poverty line, the share of non-white residents, and the CalEnviroScreen indicator of pollution vulnerability. In our primary analysis we focus on how the response of natural gas generation to renewables is distributed across population, poverty rates, and racial composition. The percentage of individuals within 3 miles of a power plant living under the poverty line and percent non-white are useful measures of potentially disadvantaged communities affected by power plant emissions. In addition, we also consider the effects across median income and pollution vulnerability as robustness checks, as well as effects using 1 and 6 mile radii. Pollution transport modeling using InMap is described further below.

### **2.1.3 Summary statistics**

Table 2 includes summary information regarding the terciles for each demographic variable along with the capacity of the generators included in each of those terciles. These terciles are constructed based on demographic data of the 241 generators - for example, a natural gas plant in a middle-class, heavily Hispanic suburb might be in the second tercile of population, third tercile of share non-white, and second tercile of share below the poverty line. The number of generators varies across terciles due to the demographic data being calculated at the plant level and some plants having more than one generator.

From Table 2 it is clear that natural gas capacity is not evenly distributed across the different demographic variables. For example, there is over 50% more natural gas capacity in the second population tercile compared to the third. As for poverty rates and the share of non-white residents, there does seem to be some variation in the distribution of natural gas capacity across the terciles, such that natural gas generation is concentrated in areas with

lower poverty rates and inconsistently distributed over racial composition.<sup>7</sup> Table 2 also shows that these different terciles represent quite different groups - the average population near natural gas plants in the first tercile is only 4,263 people, compared to an average population in the third tercile of 154,160. Similarly, natural gas plants in the first tercile for the share of non-white are in majority white areas (33% non-white on average), while natural gas plants in the third tercile are in heavily non-white areas (85% non-white).

## 2.2 Econometric strategy

Our empirical strategy to uncover the distributional benefits of emission savings from renewables at the local plant-level proceeds in three major steps, and it integrates and builds on prior econometric models developed in both the renewable electricity and environmental justice literatures (for example Fell et al. (2021) and Fowlie et al. (2012)). First, we estimate CAISO-wide responses of natural gas generation and  $\text{NO}_x$  emissions per MWh of renewable generation. Next, we estimate how that aggregate CAISO-wide response breaks down across demographic terciles. Finally, we estimate interaction models by generator that allow for heterogeneous effects across demographic characteristics (separately and jointly).

First, to evaluate how aggregate natural gas generation and  $\text{NO}_x$  emissions change in response to utility-scale solar and wind we estimate:

$$y_{hdmy} = \beta_S S_{hdmy} + \beta_W W_{hdmy} + \sum_k \sigma_k f_k(\mathbf{X}_{hdmy}) + \gamma_{hm} + \alpha_{my} + \eta_d + \epsilon_{hdmy} \quad (1)$$

where  $y_{hdmy}$  is the aggregation of generation from all natural gas generators in California for

---

<sup>7</sup> If generation and emission responses to renewables were evenly distributed by capacity across natural gas plants, then these capacity differences would proportionally drive the entirety of the response across demographics. However, as shown below, the pattern of responses that emerges is quite different than a simple capacity-based, proportional-reduction model would suggest.

hour  $h$ , day  $d$ , month  $m$ , in year  $y$ . Our explanatory variables of interest,  $S_{hdm_y}$  and  $W_{hdm_y}$ , represent hourly solar and wind generation (MWh), respectively. The function  $f_k(\mathbf{X}_{hdm_y})$  flexibly controls for hourly loads across four regions in CAISO, hourly average temperature, hourly nuclear generation, and daily natural gas price (typically quadratic in the estimations below). We include hour-by-month ( $\gamma_{hm}$ ), month-by-year ( $\alpha_{my}$ ), and day of week ( $\eta_d$ ) fixed effects and cluster standard errors at the weekly level to account for serial correlation.

Our coefficients of interest are  $\beta_S$  and  $\beta_W$ , representing the marginal change in natural gas generation or emissions per MWh of CAISO-wide utility-scale solar and wind generation, respectively. While wind and solar generation are random and intermittent, they may still be correlated with other time-varying patterns in the electricity system, and our fixed effects strategy is designed to recover causal estimates of  $\beta_S$  and  $\beta_W$ . To control for diurnal patterns in both renewable generation and electricity use, hour-by-month fixed effects  $\gamma_{hm}$  are included. While our time period is somewhat short (2018-2019), month-by-year fixed effects  $\eta_{my}$  are included to control for longer-run trends such as increasing renewable capacity and changes in the generation mix (for example, if older and less efficient gas plants retire later in the sample). Finally, day-of-week fixed effects  $\delta_d$  capture any within-week variation in the load and generation profile, though we do not a priori expect any systematic correlation between renewable generation and the day of the week.

Next, to determine how the benefits of utility-scale solar and wind are distributed across areas with different socioeconomic characteristics, we use a similar specification as in equation (1) but now aggregate hourly natural gas generation and  $\text{NO}_x$  emissions across the three demographic terciles. We then estimate the effect of solar and wind on gas generation and

NO<sub>x</sub> emissions separately for each tercile:

$$y_{hdmy}^j = \beta_S^j S_{hdmy} + \beta_W^j W_{hdmy} + \sum_k \sigma_k^j f_k(\mathbf{X}_{hdmy}) + \gamma_{hm}^j + \alpha_{my}^j + \eta_d^j + \epsilon_{hdmy}^j \quad (2)$$

where  $j = 1, 2, 3$  is an indicator for whether we are considering generators that belong to the first, second, or third tercile for a specified demographic characteristic. For example,  $\beta_W^2$  for share non-white represents the change in emissions or generation per MWh of wind for generators in the second tercile of share non-white. This is a convenient approach, as the relationships  $\sum_{j=1}^3 \beta_S^j = \beta_S$  and  $\sum_{j=1}^3 \beta_W^j = \beta_W$  should approximately hold, allowing us to decompose the wind and solar estimates from equation 1 across demographic groups.

Finally, we interact wind and solar generation with each demographic variable, separately and jointly, to test for heterogeneous effects by generator  $i$ :

$$y_{ihdmy} = \beta' \mathbf{R}_{hdmy} + \boldsymbol{\theta}' \mathbf{J}_i \mathbf{R}_{hdmy} + \sum_k \sigma_k f_k(\mathbf{X}_{ihdmy}) + \gamma_{hm} + \alpha_{my} + \eta_d + \zeta_i + \nu_{ihdmy} \quad (3)$$

where  $\mathbf{R}_{hdmy}$  is a vector for hourly wind and solar generation in CAISO,  $\mathbf{J}_i$  is a vector of demographic characteristics associated with generator  $i$ , and the key coefficients of interest  $\boldsymbol{\theta}$  will capture any heterogeneous effects of renewables by demographic characteristic. We also include generator fixed effects  $\zeta_i$ , weather station-level temperature matched to each generation within  $\mathbf{X}_{ihdmy}$ , and cluster at both the plant and weekly level.<sup>8</sup>

### 3 Results

We begin by considering the aggregate electric grid response to renewables and then decompose how that response varies by the socioeconomic characteristics of the population

---

<sup>8</sup> For the interaction models at the generator level, we focus on generation as our dependent variable. NO<sub>x</sub> emissions at the generator level are quite noisy, given the fixed effect strategy we employ, particularly for the less-variable solar generation.

surrounding natural gas plants. Following the aggregate and distributional results, we then examine the underlying mechanisms behind those findings.

### 3.1 CAISO-wide results

To establish how the overall CAISO grid responds to increases in utility-scale solar and wind, we estimate equation (1) with natural gas generation, hydroelectric generation, imports, and  $\text{NO}_x$  emissions as dependent variables. The results in the first row of Table 3 show that a 1 MWh increase in solar generation decreases gas generation by 0.38 MWh and imports by 0.43 MWh. These two effects explain the majority of the response to increased solar and suggest that a substantial portion of the benefits of increased solar occur out of state.<sup>9</sup> The second row implies a 1 MWh increase in wind generation decreases natural gas generation by 0.6 MWh and imports by 0.3 MWh. Again, natural gas and imports capture most of the generation response to increased wind generation. The results in Table 3 also suggest that wind generation decreases  $\text{NO}_x$  emissions more so than solar generation. A MWh increase in solar and wind decreases  $\text{NO}_x$  emissions by 0.011 lbs and 0.055 lbs respectively. At the average hourly levels of solar and wind generation this suggests a reduction of 142 lbs of hourly  $\text{NO}_x$  emissions due to renewable generation, with 75% of this decrease due to wind.

To further illustrate our underlying econometric strategy and the importance of the load controls, Table 4 shows the progression to our preferred specification (column 5) for estimating the natural gas generation response to increases in solar and wind generation.

The first column regresses solar and wind generation on natural gas generation with a variety

---

<sup>9</sup> This is consistent with the findings of Fell and Johnson (2021) who find a similar response to in-state renewables in California.

of fixed effects but no other controls. We then add several control variables including hourly nuclear generation, hourly load across four regions in CAISO, hourly temperature, and finally daily natural gas price. This table highlights the importance of including load variables, as the coefficients for both wind and solar are strongly negatively biased when load is excluded. This negative bias is intuitive for wind (wind is stronger overnight when load is smaller). One might assume excluding load when estimating the relationship between solar and natural gas generation would *positively* bias estimates, as load is generally higher in mid-day hours when there is more solar generation. However, in Appendix Table A.1 we demonstrate that once month-by-hour fixed effects are included, the correlation between solar and load is *negative*. This conditional negative correlation is driven by the presence of substantial behind-the-meter rooftop solar in California which decreases the grid’s hourly load during sunny hours.<sup>10</sup> Importantly, while we cannot directly estimate the effects of rooftop solar, the load variables effectively control for any confounding influence.

### 3.2 Distributional results across terciles

The above results establish that natural gas balances most of the in-state response to wind and solar in California, on the order of  $\hat{\beta}_S = 0.4$  MWh of gas per 1 MWh of solar and  $\hat{\beta}_W = 0.6$  MWh of gas per 1 MWh of wind. The distributional and EJ effects will then hinge on the demographics of where the responding natural gas plants are located within California - that is, how that 0.4 or 0.6 MWh response to solar and wind is distributed across different demographics within the state. Based on estimations of equation 2, Figures 1 and

---

<sup>10</sup> In other words, if it is a particularly sunny day for 4pm in June, then we will observe relatively higher utility-scale solar generation and relatively lower load (due to rooftop solar).

2 plot the estimated effects of solar and wind generation on natural gas generation and  $\text{NO}_x$  emissions across the different demographic terciles ( $\hat{\beta}_S^j$  and  $\hat{\beta}_W^j$ ), while Table 5 reports the coefficient and standard error estimates.

The top panels of Figures 1 and 2 show that there is a much larger generation and emission response to renewables in lower population, rural areas (first tercile of population). The effect of solar generation on natural gas generation in the first population tercile is six times larger than in the second population tercile and an order-of-magnitude larger than the estimated effect in the third population tercile. As for wind generation, the estimated reduction of gas generation in the first population tercile is roughly double of that in the second tercile and almost five times larger than in the third population tercile.

By contrast, the second and third panels of Figures 1 and 2 show that the generation and emissions response to renewables are evenly distributed across the share below the poverty line and share non-white terciles. At most, there is a slightly larger response from generators in the second poverty tercile, but this difference is not statistically significant. Thus, these estimates indicate that while wind and solar offset fossil generation and emissions roughly evenly across racial and poverty lines, fossil fuel generators in rural areas are up to an order of magnitude more responsive to renewables than fossil plants in urban areas.

### **3.3 Heterogenous effects across demographics**

Next, we estimate a series of interaction models based on equation 3. These generator-level regressions will allow us to test whether the effect of wind and solar on natural gas generation is statistically different for plants with different surrounding demographics. Given the large

responsiveness of generators in low populations areas found above, the joint interaction model will also us allow to see if, conditional on the large rural effect, there are differential effects across racial or poverty lines.

Table 6 columns 1-3 estimate interaction models separately by population, share below the poverty line, and share non-white, while column 4 estimates the interactions jointly. Similar to the tercile estimates, across columns 1-3 there is no evidence of a heterogenous effect across poverty or racial lines, and we again see that the negative effect of wind and solar on natural gas generation is largest for low population areas, and the effect attenuates as population increases. The mean population in the third population tercile is 154,160 residents, and the estimates in column (1) imply a solar marginal effect per MWh of  $-0.00187$  ( $p < 0.001$ ) and a wind marginal effect per MWh of  $-0.00095$  ( $p = 0.086$ ). In the joint interaction model in column 4, this pattern still holds when conditioned on the large rural effect, and there are no heterogenous effects along racial or poverty lines. The marginal effects for the joint interaction model at the average population of the third tercile are  $-0.000774$  ( $p = 0.375$ ) for solar and  $-0.00094$  ( $p = 0.505$ ) for wind.

### **3.4 Mechanisms - transmission or merit-order effects?**

The above results indicate a clear pattern: The first-order distributional effect of renewable generation on local emissions is that residents who live in less populated areas of California are benefitting from reduced fossil fuel generation. There are a number of possible mechanisms that could lead to rural natural gas generators and emissions responding more strongly to renewable generation. Broadly speaking, we will explore two potential mechanisms, a

*transmission effect* and a *merit order effect*.<sup>11</sup> A *transmission effect* would be a result of transmission constraints and congestion - natural gas generators closest to the sources of renewable generation may simply be the only generators able to respond. Prior work in California (Davis and Hausman 2016) and other states (Fell et al. 2021) has demonstrated the potential for congestion to alter the spatial pattern of generation, and most renewable generation in California is in central and eastern rural areas of the state. Alternatively, a *merit order effect* would arise if natural gas generators who respond to renewables have higher marginal costs, and thus are being pushed off the margin by renewables (Fell and Kaffine 2018). If these high marginal cost plants also happen to be located in rural areas, then this would be consistent with the results above. Below, we consider two key components of generator marginal cost: the heat rate (efficiency) of the generator and the fuel price paid.

### 3.4.1 Interactions with plant characteristics

We begin by estimating heterogeneous generator-level responses as a function of three plant characteristics: proximity to renewables, heat rate, and fuel price. To determine if generators in close proximity to renewables respond more via a transmission effect, we interact wind ( $W_{hdmy}$ ) and solar ( $S_{hdmy}$ ) with the corresponding wind and solar capacity within 75 km of each generator. Similarly, to determine if heat rates are an important predictor of generator response, we interact each generator's heat rate averaged over the sample period with wind

---

<sup>11</sup> A simple conceptual model of wholesale electricity markets such as CAISO is that generators are dispatched in order of ascending marginal cost (the merit order), until demand (load) is met. This marginal unit sets the market clearing price - in the absence of transmission constraints, this means a generator in Long Beach receives the exact same price for its electricity as a generator in Sacramento. However, once transmission lines reach their capacity and congestion occurs, local marginal prices begin to spatially diverge. These prices may even be negative at times in areas with lots of renewables and insufficient transmission capacity to move the power to higher demand areas.

and solar generation.<sup>12</sup> Finally, the other important component of a generator’s marginal cost is the price paid for fuel. In California there is spatial variability in the price paid for natural gas, due to the prominent pipeline in the PG&E area referred to as the “backbone”. Thus, we interact an indicator of whether the generator is a “non-backbone” (NBB) plant (and therefore has higher fuel prices) with wind and solar generation.<sup>13</sup>

As such, we first estimate a set of generator-level models, similar to equation 3.<sup>14</sup> The key distinction is that instead of reflecting local demographics, the interaction with vector  $\mathbf{J}_i$  captures the plant characteristics described above  $\{SolarCap, WindCap, HeatRate, NBB\}$ . Note, this first set of regressions will simply establish which plant characteristics are associated with a more vigorous response to wind and solar generation, and we will then examine whether plants with those characteristics are more likely to be located in rural areas.

The results of this interaction model are shown in Table 7. The coefficients on the interaction terms  $Solar * SolarCap$  and  $Wind * WindCap$  show that natural gas generators with an additional 1000 MW of solar or wind capacity within 75 km are more responsive to increased solar or wind generation. This roughly equates to a one standard deviation increase in the nearby capacity of wind (840 MW) or solar (1070 MW) is associated with a

---

<sup>12</sup> The heat rate is the heat input (fuel) divided by the amount of generation (electricity), both of which are provided by the EPA CEMS database, and it is a key component of a generator’s marginal cost. Higher heat rate plants are less efficient and thus have higher marginal costs.

<sup>13</sup> Generators in PG&E are identified as either “backbone” or “non-backbone” generators. The non-backbone generators must pay a significant tariff to receive natural gas from the pipeline, while the backbone generators can avoid these fees (<https://docs.cpuc.ca.gov/PublishedDocs/Efile/G000/M191/K497/191497887.PDF>). In fact, the substantial tariff paid by non-backbone generators makes their fuel price more expensive than generators outside of PG&E that utilize a different pipeline.

<sup>14</sup> Note, as in Table 6, generator level estimates result in much smaller coefficient estimates for solar and wind. For reference, regressing generator-level generation on hourly wind and solar, without interactions, yields a coefficient of -0.0024 for wind and -0.0028 for solar (see Appendix Table A.3). With 241 generators, the aggregate effects of wind and solar on natural gas generation are -0.58 and -0.67, respectively, which are fairly similar to results found in the aggregated regression in Table 3.

40% larger response from a natural gas generator.<sup>15</sup> Next, the coefficients on the interaction terms  $Solar * HeatRate$  and  $Wind * HeatRate$  show that natural gas generators with higher heat rates are more responsive to solar (negative), but not to wind (positive), though neither are statistically significant. Finally, the coefficients on the interaction terms  $Solar * NBB$  and  $Wind * NBB$  show that non-backbone generators in PG&E are actually less responsive to solar and wind, though again, neither are statistically significant.<sup>16</sup>

### 3.4.2 Plant location and plant characteristics

The interaction model above demonstrated that natural gas plants are more responsive to solar if they are located near more solar capacity and are more responsive to wind if they are located near more wind capacity. We now examine the spatial overlap between natural gas plants located in areas with low population (first tercile of population) and these more responsive plants that are near renewable capacity. To do this, we allocate natural gas plants to terciles based on the amount of nearby wind or solar capacity.

Table 8 shows that of the 81 generators in the lowest population tercile, 72% are in the second or third solar capacity tercile (46% in the largest tercile) and 80% in the second or third wind capacity tercile.<sup>17</sup> By contrast, there are few inefficient heat rate plants (third tercile) in the first tercile of population, and the most inefficient plants tend to be in the second and third terciles of population.<sup>18</sup> Finally, it does not appear that non-backbone

---

<sup>15</sup> The choice of 75 km is somewhat arbitrary, but strikes a reasonable balance between capturing “close” renewable capacity and ensuring enough non-zero observations to have statistical power. Appendix Figure A.2 displays point estimates for alternative distances from 30-100 km, which as expected finds noisier estimates for smaller distances and attenuated point estimates for larger distances.

<sup>16</sup> The positive interaction terms are somewhat surprising, as this implies that these higher cost plants are actually less responsive to renewables. However, while it may be true non-backbone plants are likely to have higher fuel costs, these plants may also differ in other ways that make them less responsive.

<sup>17</sup> Scatterplot between population within 3 miles and solar/wind capacity in Appendix Figure A.3

<sup>18</sup> Scatterplot between population and heat rate provided in Appendix Figure A.4

plants are overrepresented in the lowest population tercile - about a quarter of generators across California are non-backbone, and about a quarter of generators in the first population tercile are non-backbone.

Taken together, the results for wind and solar proximity from Tables 7 and 8 are strong evidence of a *transmission effect*. That is, the effects of renewable generation on natural gas generators are concentrated in lower population terciles due to the proximity of those generators to wind and solar plants. On the other hand, there is very little evidence for a *merit order effect*, either in terms of heat rates or fuel costs for non-backbone plants.

### 3.4.3 Price effects of congestion from wind and solar generation

The preceding sections established that natural gas generators near renewable capacity are both more responsive to renewable generation and more likely to be located in lower population areas, indicative of a *transmission effect* driving our main findings. To further test this mechanism, we examine the extent to which wind and solar generation are creating local transmission congestion and driving down the electricity prices received by nearby natural gas generators. If transmission is the key mechanism behind our main findings, we would expect to see depressed prices due to wind and solar generation most prominently in the first tercile of population.

We collect hourly nodal prices within CAISO, both the local marginal prices (LMP) and the separately reported marginal congestion cost (MCC), for all generators in CAISO.<sup>19</sup> We focus on the MCC, which is positive at a node (increases price received) if adding power to the grid at that node would alleviate congestion and negative at a node (decreases price

---

<sup>19</sup> The local marginal price at a node is the system-wide energy cost to meet demand, adjusted by the MCC at that node as well as costs associated with line losses.

received) if adding power to the grid at that node exacerbates congestion. Under extreme congestion, the congestion cost may be sufficiently negative that nodal prices are negative. We estimate a tercile-specific model similar to equation 2, but with the dependent variable as the nodal hourly marginal congestion cost  $C_{nhdmy}$ . This model is estimated at the nodal level as there are a small number of gas generators that have the same node (and thus receive the same price), and the nodes are grouped into demographic terciles according to the corresponding generators.

The effect of wind and solar generation on nodal marginal congestion costs by demographic tercile is shown in Table 9. The first specification includes the full set of observations and finds relatively noisy, insignificant effects of solar on prices across terciles, while for wind, there is a consistent pattern of larger price reductions (negative estimates) for nodes in the first population tercile. One feature of congestion costs is that they can be quite extreme (negative or positive), and so the second specification restricts the sample by dropping the most negative 1% and most positive 1% of observations. Despite dropping only 20 observations, the point estimates for solar in particular are much sharper, with the largest and most significant congestion effects occurring in the first tercile of population. Wind also has the largest and most significant effects in the first tercile. Finally, in the third specification we restrict attention to daytime hours (8am-6pm), which again shows concentrated price effects in the first tercile of population. Taken together with the renewable proximity results, the evidence suggests that transmission is the key mechanism that explains the strong effect of renewables on generation and emissions from gas generators in rural, less densely populated areas of California.

### 3.5 Pollution dispersal

The analysis thus far considers the demographics near fossil fuel plants that respond to renewables. While this likely captures many of the acute, local impacts from emissions, it is also true that pollution dispersal may be important (Hernandez-Cortes and Meng 2023; Qiu et al. 2022).<sup>20</sup> We use the InMap model (Tessum et al. 2017), a computationally-inexpensive alternative to more comprehensive atmospheric chemistry models, to capture the spatial distribution of pollution reductions due to renewables. First, we use InMap to generate base levels of PM 2.5 using pre-built emission files based on 2005 annual national emissions (e.g NO<sub>x</sub>, SO<sub>2</sub>). InMap translates these emission inputs into annual PM 2.5 concentrations over a variable grid that uses smaller grid sizes (higher resolution) in urban areas. There are 2,657 grids for California in total, and InMap includes Census population and race/ethnicity data for each grid. Next, we translate our econometric estimates in Table 6 into plant-level annual emission changes due to average annual wind and solar generation (column (1) with the statistically significant population interaction is reported below, with column (4) analyzed as a robustness check).<sup>21</sup> Finally, these changes in emissions are added into InMap on top of the base emissions to determine the change in PM 2.5 concentrations.

Figure 3 displays the change in total ground-level PM 2.5 across California due to utility-scale renewables. Consistent with the plant-level estimates based on 3-mile radii, reductions

---

<sup>20</sup> Dispersion is likely particularly important over geographies with highly varied populations such as the NO<sub>x</sub> and SO<sub>2</sub> RECLAIM program in the Los Angeles area that began in 1994 and is studied in Fowlie et al. (2012) and Grainger and Ruangmas (2018). However, this may be less important in our context given that the primary heterogeneous effect we find is between rural (Central Valley) and urban areas (coastal), and the general wind pattern will tend to move pollution eastward (to even more rural and empty areas).

<sup>21</sup> We compute changes in plant-level NO<sub>x</sub> emissions directly from the table estimates, while the change in PM 2.5 emissions is derived from the generation responses by using an average PM 2.5 emissions rate for natural gas generators in California of 0.03 lb/MWh - See [https://www.epa.gov/sites/production/files/2020-07/documents/draft\\_egrid\\_pm\\_white\\_paper\\_7-20-20.pdf](https://www.epa.gov/sites/production/files/2020-07/documents/draft_egrid_pm_white_paper_7-20-20.pdf).

in pollution occur primarily in the lower-population interior regions of California, though there are some reductions in higher-population areas of Southern California. However, in contrast to the plant-level estimates, we do find evidence of greater pollution reductions in areas with a greater share of non-white households. We calculate that a higher share of emission reductions accrued to non-white households (66%) compared to their overall population share (61%). Additional regression analysis in Appendix Table A.4 and Appendix Figure A.5 confirms larger reductions in pollution concentrations in both lower population areas and areas with a greater share of non-white households. So while plant-level generation and emission responses to renewables are roughly equal across areas with differing local shares of non-white households, the InMap pollution dispersion analysis provides evidence that renewables may be contributing to EJ goals via larger pollution reductions in areas with a greater share of non-white households.

### **3.6 Robustness checks and extensions**

Finally, we consider a series of robustness exercises and extensions of the model above. In particular, we examine alternative demographic variables, effects across different utilities within California, and alternative radii for determining the demographics associated with a generator. Two alternative demographic characteristics that may be of interest are median income and CalEnviroScreen scores. The CalEnviroScreen index incorporates both the geographical susceptibility to pollution as well as the vulnerability of the population. Higher CalEnviroScreen index values indicate higher vulnerability to pollution due to medical factors, such as prevalence of heart disease, as well as socioeconomic factors (educational

attainment, poverty, unemployment, etc.).<sup>22</sup> Summary statistics in Appendix Table A.5 show that natural gas capacity is roughly evenly distributed across terciles of median income, while there is more gas capacity in the lowest tercile of CalEnviroScreen.

The results across CalEnviroScreen terciles (Appendix Figures A.6 and A.7, Appendix Table A.6) show modestly larger generation and emissions reductions in areas of average susceptibility to pollution (second tercile). The effects across median income terciles are more idiosyncratic, as there are larger decreases in natural gas generation in the lowest tercile of median income, but larger decreases in NO<sub>x</sub> emissions in the second tercile.<sup>23</sup> The larger generation response for plants in areas with low median income, but not higher poverty share, may be a bit surprising; however, this follows from Appendix Table A.7 and A.8, as median income and population are correlated, while poverty line share and population are not. That is, rural areas may have lower median incomes, but not necessarily more individuals living below the poverty line. The consistent emission reductions in population area suggests the demographic attributes of the individuals who live in rural areas will dictate which groups benefit most from increased utility-scale solar and wind.<sup>24</sup>

Next, we examine emissions responses for the three main utilities within CAISO.<sup>25</sup> The two largest utilities, PG&E and SCE, respectively serve northern California and most of

---

<sup>22</sup> For CalEnviroScreen details, see <https://oehha.ca.gov/media/downloads/calenviroscreen/report/ces3report.pdf>. Median income measures may not reflect a disadvantaged community as well as the share below the poverty line since the median income can still be high in areas with higher poverty rates, depending on the distribution of income.

<sup>23</sup> One possible explanation for this discrepancy is due to the average emission rate of NO<sub>x</sub> emissions for generators across median income terciles. The average in the first median income tercile is 0.035 lbs/mmBtu while the average in the second tercile is 0.07 lbs/mmBtu, implying generators in the lowest median income tercile are substantially cleaner per unit of fuel input.

<sup>24</sup> For example, in Appendix Table A.10 a jointly estimated interaction model finds no evidence of a heterogeneous effect across median income conditional on a population interaction term also being included, suggesting population is the key factor.

<sup>25</sup> VEA (Valley Electric Association) is a small electric cooperative that joined California ISO in 2013. Average hourly load in this region is roughly 70 MWh (<1% of CAISO's hourly load).

southern California, and SDG&E serves the San Diego area (see Appendix Table A.11 for summary statistics). We estimate the effect of solar and wind generation across all five demographic characteristics for each utility area (Appendix Figures A.8-A.12). In Appendix Table A.12, decreases in natural gas generation in response to renewables are again concentrated in less populated areas across all three utilities. The coefficients for  $\text{NO}_x$  have a less clear distribution, with larger  $\text{NO}_x$  emission reductions from wind in lower population areas, but more evenly distributed and less statistically significant emission reductions from solar.

The results across poverty share terciles are provided in Appendix Table A.13 and are consistent with the correlations between population and poverty rates in each utility (Appendix Table A.8). In PG&E there is no consistent pattern in generator response across poverty terciles, corresponding to a weak relationship between population size and poverty rates in PG&E. In SCE, there is a stronger, negative correlation between population and poverty rates (low population areas generally have higher poverty rates), which is consistent with the largest effect of wind and solar in the highest poverty rate tercile. Lastly in SDG&E, the relationship between population and poverty share is positive, and the generators that respond the most to solar and wind in SDG&E are in the lowest poverty rate tercile. A similar pattern emerges for median income in Appendix Table A.14. Positive correlations between population and median income in PG&E and SCE correspond to larger responses in the lowest income tercile, while the negative correlation between population and median income in SDG&E corresponds to largest effects in the highest median income tercile. This again suggests correlations between population and other demographic characteristics drive the effects of renewables on those demographic characteristics.

Finally, an important feature of our plant-level analysis is that we are analyzing demo-

graphics within a 3-mile radius of natural gas generators (a radius-based approach). This 3-mile radius represents a plausible set of local residents most acutely affected by fossil fuel plant operations, and conveniently is the (approximate) radius used in the CAISO 20-year Transmission Outlook (2.5 miles) when considering plant closures near disadvantaged communities. While our InMap analysis provides useful insight into the spatial distribution of pollution reductions, an additional useful robustness check for radius-based approaches is to examine alternative radii, and so we re-estimate our key Figure 1 with 1-mile and 6-mile radii in Appendix Figures A.13-A.15. Again, there is a strong generation response from low population gas plants relative to higher population plants, while responses across poverty and racial terciles are roughly equivalent.

## 4 Economic and policy implications

### 4.1 Monetized benefits of emission reductions

The above estimations reveal a consistent pattern of utility-scale renewables reducing generation and emissions in less populated areas of California. As a back of the envelope exercise, we now consider the distribution of the monetized benefits associated with emissions reductions of  $\text{NO}_x$  and  $\text{PM}_{2.5}$ .<sup>26</sup> With the CEMS data from the EPA database above, we are able to directly estimate the hourly changes in  $\text{NO}_x$  emissions by tercile in response to solar and wind generation (Table 5) and approximate changes in  $\text{PM}_{2.5}$  emissions using the average emissions rate of  $\text{PM}_{2.5}$  for natural gas generators in California of 0.03 lb/MWh.

---

<sup>26</sup> There will also be reductions in carbon dioxide emissions but since this is a global pollutant, we are not concerned with the distribution of carbon dioxide emissions across different areas.

We first aggregate the total annual decrease in both  $\text{NO}_x$  and  $\text{PM}_{2.5}$  emissions by assuming a constant marginal emissions offset rate. In 2019, there was a total of 28 million MWh of solar generation and 15.9 million MWh of wind generation. We use these annual amounts, along with our coefficient estimates to approximate annual decreases in  $\text{NO}_x$  and  $\text{PM}_{2.5}$  emissions due to solar and wind generation by tercile. Not all reductions in emissions are equally beneficial, and so we obtain county-specific damages per ton from Holland et al. (2016) in order to construct tercile-specific damages by taking a capacity-weighted average of the county damages. Each tercile's pollution damage value per ton is thus dependent on the capacity of natural gas generation in each county and the value of that county's damage per ton. These values are provided in Appendix Table A.17.<sup>27</sup>

Table 10 uses the 2019 annual solar and wind generation, the estimated coefficients for the effect of wind and solar on  $\text{NO}_x$  and natural gas generation, the average rate of  $\text{PM}_{2.5}$  emissions per MWh, and county-weighted damages by pollutant and tercile to calculate the avoided emissions and corresponding avoided damages for  $\text{NO}_x$  and  $\text{PM}_{2.5}$  in each population tercile. The benefits of solar and wind are similar in the first and second population tercile, roughly \$18 million and \$23 million in total, respectively. Although the decreases in  $\text{NO}_x$  and  $\text{PM}_{2.5}$  emissions are roughly 50% larger in the first tercile, the damages per ton of emissions in the second tercile are around twice as large (due to the higher population density in those areas). This results in slightly higher avoided emissions damages in the second tercile than the first. By contrast, the benefit of solar and wind generation is much smaller in the third population tercile at around \$7 million. Thus, despite larger damages per ton of emissions

---

<sup>27</sup> As expected, a ton of emissions reductions in the first tercile has less monetary benefit than a ton of emissions reductions in the third tercile, simply because the damages per ton as computed in Holland et al. (2016) correlate strongly with population.

avoided for third tercile plants, only around 20% of the monetized benefits from emission reductions from renewables accrue to the high population density areas in California.

## 4.2 Impacts on plant profitability

As noted above, CAISO's 20-year transmission outlook plan assumed natural gas plants near disadvantaged communities, many of which are in the populated Bay Area and LA Basin, would be retired first. However, given that the bulk of those identified plants are in the highest population tercile, simply relying on economic retirement from increased renewable share is unlikely to lead those plants to retire. To illustrate, as a back-of-the-envelope exercise we calculate profit losses for natural gas plants assuming a 1000 MWh increase in solar generation from existing sites.<sup>28</sup> Combining heterogeneous quantity responses to solar from Table 6, and heterogeneous congestion price responses to solar from Appendix Table A.19, we then determine the average changes in revenues, costs and profits by demographic tercile. Rural natural gas plants in the first population tercile would see a 4.7% decline in profitability, compared to a 3.7% decline in the second population tercile and only a 1.9% decline in the third population tercile.<sup>29</sup> This suggests that increasing renewable share will primarily put economic pressure on rural fossil plants to retire, and thus other policy levers may be necessary to encourage retirement of plants near disadvantaged communities, consistent with CAISO's 20-year transmission outlook plan.

---

<sup>28</sup> Essentially, this assumes the additional solar generation (about a one-third increase) is being generated in areas with existing solar capacity and thus would have similar impacts on the spatial pattern of reductions in natural gas generation. We also abstract from different heat rates and other plant-specific characteristics in order to focus on quantity and price impacts in lower and higher population areas.

<sup>29</sup> Note this profit loss calculation emphasises the relative changes as it only includes the congestion price effects, and thus ignores any change in the overall system energy price due to renewables.

### 4.3 Policy implications

A number of important policy implications for clean electricity standards and transmission policy follow from the above analysis.<sup>30</sup> A majority of US states have adopted renewable portfolio standards (RPS) that mandate a certain percentage of renewable electricity be produced by state utilities, in part because they are touted to reduce local emissions (Bento et al. 2018), and there is ongoing policy momentum for some form of a federal clean electricity standard. While carbon markets have been criticized for failing to reduce local emissions and improve local air quality, aside from Qiu et al. (2022) there is limited empirical evidence for the distributional effects of clean energy standards, or the mechanisms that drive them. Our results suggest that, at the local plant-level, plant-level reductions in fossil generation and emissions are uncorrelated with EJ goals for poverty or race, while pollution transport modelling does suggest some beneficial reduction in ground-level PM 2.5 for disadvantaged communities. By contrast, utility-scale renewables do deliver large reductions in emissions for rural populations, both at the very local plant level and through pollution transport.

Several proposed and existing standards have ambitious targets that would require large increases in renewable capacity, and it is natural to wonder whether our findings will hold for such large increases in renewable capacity. While it is beyond the scope of this paper to envision scenarios with extremely high renewable penetration, in Appendix Table A.18 we estimate our main tercile specification on hours with above and below 20% renewable share. Estimates in high renewable share hours continue find a much larger response from gas plants in the least populated areas, which suggests our findings are likely to hold at

---

<sup>30</sup> Of course, local air quality is not the only distributional consideration at stake for various energy policies. Policies can also differentially affect energy prices, the labor force, and total carbon emissions, which can each have their own distributional implications.

least in the short to medium run.<sup>31</sup> A second line of inquiry is whether or not our findings would hold for other states or regions of the US. It is been noted in the context of Texas and the upper Midwest that renewables are located in western, more rural areas and are often transmission constrained, preventing the movement of renewable electricity from renewable-rich areas to high-demand population centers further east (Fell et al. 2021). This suggests that similar distributional and EJ patterns with respect to population would exist in the important wind belt in the central US, with wind and solar tending to offset rural emissions - impacts on poverty share and non-white households would then be driven by correlations with population levels.<sup>32</sup>

Our findings also have important implications for infrastructure and transmission planning. Billions of dollars are spent every year by utilities on transmission expansion, and there are numerous projects to connect renewable-rich areas to demand centers that are in the works or completed (e.g. the Competitive Renewable Energy Zone - CREZ - lines in Texas). While these quasi-public or private transmission plans often focus on market arbitrage opportunities (LaRiviere and Lyu 2022), our results show that transmission planning also has EJ implications by changing the distribution of air quality improvements. While we observe a particular pattern in California of emission responses to renewables (rural effects driven by transmission and congestion) this reflects the current transmission infrastructure system. In theory, this pattern is something policymakers could alter, for example by encouraging transmission expansions that facilitate moving renewable energy to offset power

---

<sup>31</sup> Of course, given that dirty fossil generation is concentrated in disadvantaged communities, a 100% clean electricity standard would necessarily have positive EJ outcomes to the extent those communities would see proportionately larger improvements in emissions.

<sup>32</sup> This is an interesting contrast with Holland et al. (2019) who note that electric vehicles tend to move emissions generation out of cities and into more rural areas where there are more fossil power plants.

plants in disadvantaged communities, which in turn could improve EJ outcomes.

## 5 Conclusions

With the growing concerns over climate change and local air pollution from the electricity sector, there has been a nationwide push to replace carbon- and emissions-intensive energy sources with renewable energy. This, coupled with the drastic decrease in the costs of solar panels and wind turbines, has resulted in a dramatic increase in renewable electricity generation. Although a reduction in global emissions benefits everyone, the corresponding decrease in other local emissions is felt much more locally. This paper answers the EJ question of who benefits from these reduced local emissions from renewable electricity generation, and explores whether transmission or merit order considerations drive the distributional outcomes.

First, we focus on which natural gas generators in California respond to utility-scale solar and wind generation. Using demographic data on the individuals who live within 3 miles of each generator, we are able to estimate the effect of solar and wind on natural gas generation and emissions across demographic terciles of population, poverty line share, and non-white share. Natural gas plants in less densely populated areas have the largest generation and emission response to solar and wind generation. Natural gas generators in the first tercile of population are up to an order of magnitude more responsive to renewables than gas generators in the third population tercile. In contrast, we find no evidence of differential effects across racial or poverty lines. Pollution transport modeling via InMap confirms the larger reductions in ground-level PM 2.5 in rural areas, but in contrast to the plant-level response estimates, pollution dispersion results suggest that areas with greater

shares of non-white households benefited more from pollution reductions.

Second, we show that transmission is the key mechanism behind the large rural response. In particular, we find that gas generators with more solar and wind capacity within 75 km are substantially more responsive to solar and wind generation, and that these gas generators tend to be located in rural areas near the solar and wind resources in the central valley and deserts of eastern California. We also show wind and solar disproportionately drive down electricity prices in the first population tercile via local congestion prices, lowering the prices paid (and thus the incentives to generate electricity) for gas generators in rural areas. Transmission ultimately dictates which generators respond to renewables, and thus the distributional and EJ implications tend to follow the demographics of who lives near the responding rural generators.

Finally, these results provide useful insight into ongoing policy debates related to clean electricity standards and grid transmission investment. California may be targeting power plants within 2.5km of disadvantaged communities for retirement, but we find that simply relying on increasing shares of renewable generation to push those gas plants into retirement is unlikely to be successful. While we focus on California, our finding that those who benefit most from reduced fossil emissions are those who live in rural areas closest to wind and solar resources is likely to hold broadly across the US, at least for the short-to-medium run. In sum, under the current transmission network, most of the physical and monetized benefits of emissions reductions flow to lower population areas, neither necessarily helping nor hindering EJ outcomes across race or poverty lines. However, policies that increase transmission capacity to disadvantaged communities may change the EJ outcomes from renewables.

## References

- Baker, E., M. Fowlie, D. Lemoine, and S. S. Reynolds (2013). The economics of solar electricity. *Annual Review of Resource Economics* 5(1), 387–426.
- Banzhaf, S., L. Ma, and C. Timmins (2019). Environmental justice: The economics of race, place, and pollution. *Journal of Economic Perspectives* 33(1), 185–208.
- Bento, A., M. Freedman, and C. Lang (2015). Who benefits from environmental regulation? evidence from the clean air act amendments. *Review of Economics and Statistics* 97(3), 610–622.
- Bento, A. M., T. Garg, and D. Kaffine (2018). Emissions reductions or green booms? general equilibrium effects of a renewable portfolio standard. *Journal of Environmental Economics and Management* 90, 78–100.
- Borenstein, S. and L. W. Davis (2016). The distributional effects of us clean energy tax credits. *Tax Policy and the Economy* 30(1), 191–234.
- Callaway, D. S., M. Fowlie, and G. McCormick (2018). Location, location, location: The variable value of renewable energy and demand-side efficiency resources. *Journal of the Association of Environmental and Resource Economists* 5(1), 39–75.
- Chapman, A. J., B. C. McLellan, and T. Tezuka (2018). Prioritizing mitigation efforts considering co-benefits, equity and energy justice: Fossil fuel to renewable energy transition pathways. *Applied Energy* 219, 187–198.
- Cullen, J. (2013). Measuring the environmental benefits of wind-generated electricity. *American Economic Journal: Economic Policy* 5(4), 107–133.

- Currie, J., J. Voorheis, and R. Walker (2020). What caused racial disparities in particulate exposure to fall? new evidence from the clean air act and satellite-based measures of air quality. Technical report, National Bureau of Economic Research.
- Currie, J. and R. Walker (2011). Traffic congestion and infant health: Evidence from e-zpass. *American Economic Journal: Applied Economics* 3(1), 65–90.
- Cushing, L., D. Blaustein-Rejto, M. Wander, M. Pastor, J. Sadd, A. Zhu, and R. Morello-Frosch (2018). Carbon trading, co-pollutants, and environmental equity: Evidence from california’s cap-and-trade program (2011–2015). *PLoS medicine* 15(7), e1002604.
- Davis, L. and C. Hausman (2016). Market impacts of a nuclear power plant closure. *American Economic Journal: Applied Economics* 8(2), 92–122.
- Deryugina, T., G. Heutel, N. H. Miller, D. Molitor, and J. Reif (2019). The mortality and medical costs of air pollution: Evidence from changes in wind direction. *American Economic Review* 109(12), 4178–4219.
- Deschênes, O., M. Greenstone, and J. S. Shapiro (2017). Defensive investments and the demand for air quality: Evidence from the nox budget program. *American Economic Review* 107(10), 2958–89.
- Fell, H. and J. X. Johnson (2021). Regional disparities in emissions reduction and net trade from renewables. *Nature Sustainability* 4(4), 358–365.
- Fell, H. and D. T. Kaffine (2018). The fall of coal: Joint impacts of fuel prices and renewables on generation and emissions. *American Economic Journal: Economic Policy* 10(2), 90–116.

- Fell, H., D. T. Kaffine, and K. Novan (2021). Emissions, transmission, and the environmental value of renewable energy. *American Economic Journal: Economic Policy* 13(2), 241–72.
- Fowle, M., S. P. Holland, and E. T. Mansur (2012). What do emissions markets deliver and to whom? evidence from southern california’s nox trading program. *American Economic Review* 102(2), 965–93.
- Gonzales, L. E., K. Ito, and M. Reguant (2022). The dynamic impact of market integration: Evidence from renewable energy expansion in chile. Technical report, National Bureau of Economic Research.
- Grainger, C. and T. Ruangmas (2018). Who wins from emissions trading? evidence from california. *Environmental and Resource Economics* 71(3), 703–727.
- Harris, R. I. and T. E. Dauwalter (2022). Distributional benefits of rooftop solar capacity. *Journal of the Association of Environmental and Resource Economists*.
- Hernandez-Cortes, D. and K. C. Meng (2023). Do environmental markets cause environmental injustice? evidence from california’s carbon market. *Journal of Public Economics* 217, 104786.
- Holland, S. P., E. T. Mansur, N. Z. Muller, and A. J. Yates (2019). Distributional effects of air pollution from electric vehicle adoption. *Journal of the Association of Environmental and Resource Economists* 6(S1), S65–S94.
- Holland, S. P., E. T. Mansur, N. Z. Muller, A. J. Yates, et al. (2016). Are there environmental benefits from driving electric vehicles? The importance of local factors. *American Economic Review* 106(12), 3700–3729.

- Kaffine, D. T., B. J. McBee, and J. Lieskovsky (2013). Emissions savings from wind power generation in Texas. *Energy Journal* 34(1), 155–175.
- LaRiviere, J. and X. Lyu (2022). Transmission constraints, intermittent renewables and welfare. *Journal of Environmental Economics and Management* 112, 102618.
- Li, Z., D. M. Konisky, and N. Zirogiannis (2019). Racial, ethnic, and income disparities in air pollution: A study of excess emissions in texas. *PloS one* 14(8), e0220696.
- Lukanov, B. R. and E. M. Krieger (2019). Distributed solar and environmental justice: Exploring the demographic and socio-economic trends of residential pv adoption in california. *Energy Policy* 134, 110935.
- Mansur, E. T. and G. Sheriff (2021). On the measurement of environmental inequality: Ranking emissions distributions generated by different policy instruments. *Journal of the Association of Environmental and Resource Economists* 8(4), 721–758.
- Millstein, D., R. Wiser, M. Bolinger, and G. Barbose (2017). The climate and air-quality benefits of wind and solar power in the United States. *Nature Energy* 6, 17134.
- Mueller, J. T. and M. M. Brooks (2020). Burdened by renewable energy? a multi-scalar analysis of distributional justice and wind energy in the united states. *Energy Research & Social Science* 63, 101406.
- Muller, N. Z. and R. Mendelsohn (2009). Efficient pollution regulation: Getting the prices right. *American Economic Review* 99(5), 1714–1739.
- Novan, K. M. (2015). Valuing the wind: Renewable energy policies and air pollution avoided. *American Economic Journal: Economic Policy* 7(3), 291–326.

- Qiu, M., C. M. Zigler, and N. E. Selin (2022). Impacts of wind power on air quality, premature mortality, and exposure disparities in the united states. *Science Advances* 8(48), eabn8762.
- Rivera, N. M., C. Ruiz-Tagle, and E. Spiller (2021). The health benefits of solar power generation: Evidence from chile. *Environmental Defense Fund Economics Discussion Paper Series, EDF EDP*, 21–02.
- Schlenker, W. and W. R. Walker (2016). Airports, air pollution, and contemporaneous health. *Review of Economic Studies* 83(2), 768–809.
- Sexton, S., A. J. Kirkpatrick, R. I. Harris, and N. Z. Muller (2021). Heterogeneous solar capacity benefits, appropriability, and the costs of suboptimal siting. *Journal of the Association of Environmental and Resource Economists* 8(6), 1209–1244.
- Shapiro, J. S. and R. Walker (2021). Where is pollution moving? environmental markets and environmental justice. In *AEA Papers and Proceedings*, Volume 111, pp. 410–14.
- Tessum, C. W., J. D. Hill, and J. D. Marshall (2017). Inmap: A model for air pollution interventions. *PloS one* 12(4), e0176131.
- Zivin, J. S. G., M. J. Kotchen, and E. T. Mansur (2014). Spatial and temporal heterogeneity of marginal emissions: Implications for electric cars and other electricity-shifting policies. *Journal of Economic Behavior and Organization* 107, 248–268.

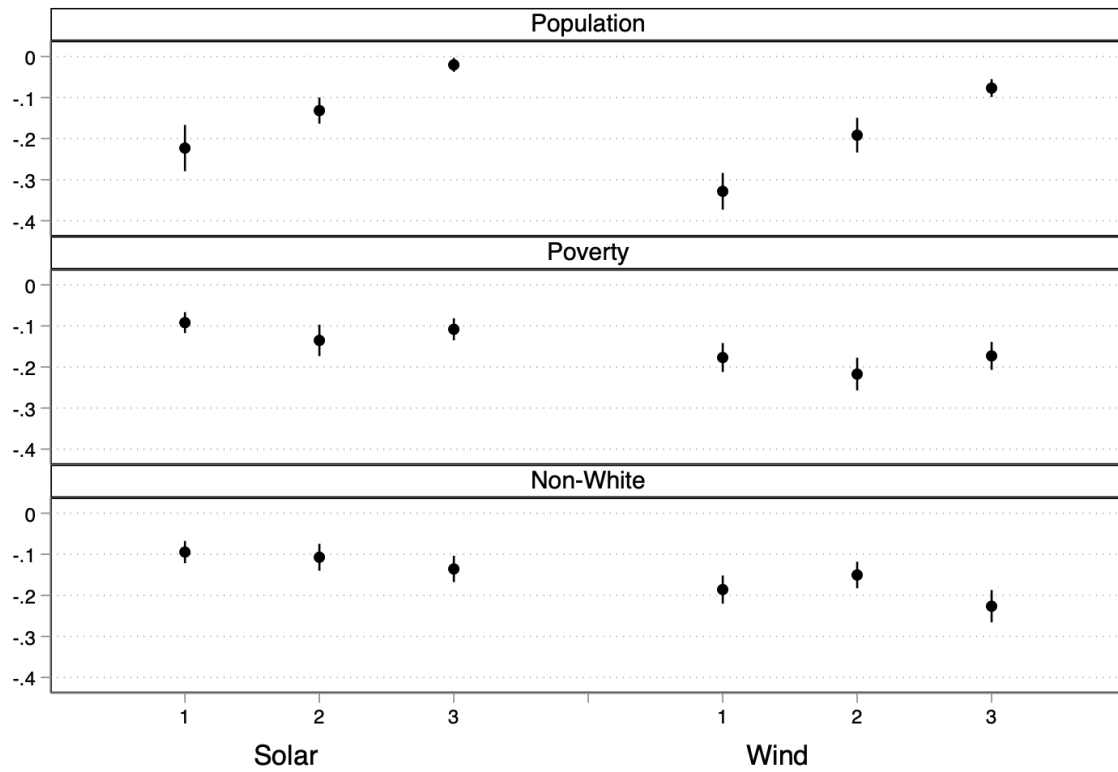


Figure 1: Effect of Solar and Wind on Natural Gas Generation across Demographic Terciles

Notes: Coefficients represent change in hourly CAISO-wide MWh generation from natural gas generators per MWh of solar or wind generation, in each respective demographic tercile. All regressions include hour-by-month, month-by-year, and day-of-week fixed effects as well as linear controls for nuclear generation and quadratic controls for temperature, natural gas price, and hourly load for four regions in CAISO. Error bars constructed from standard errors clustered by week.

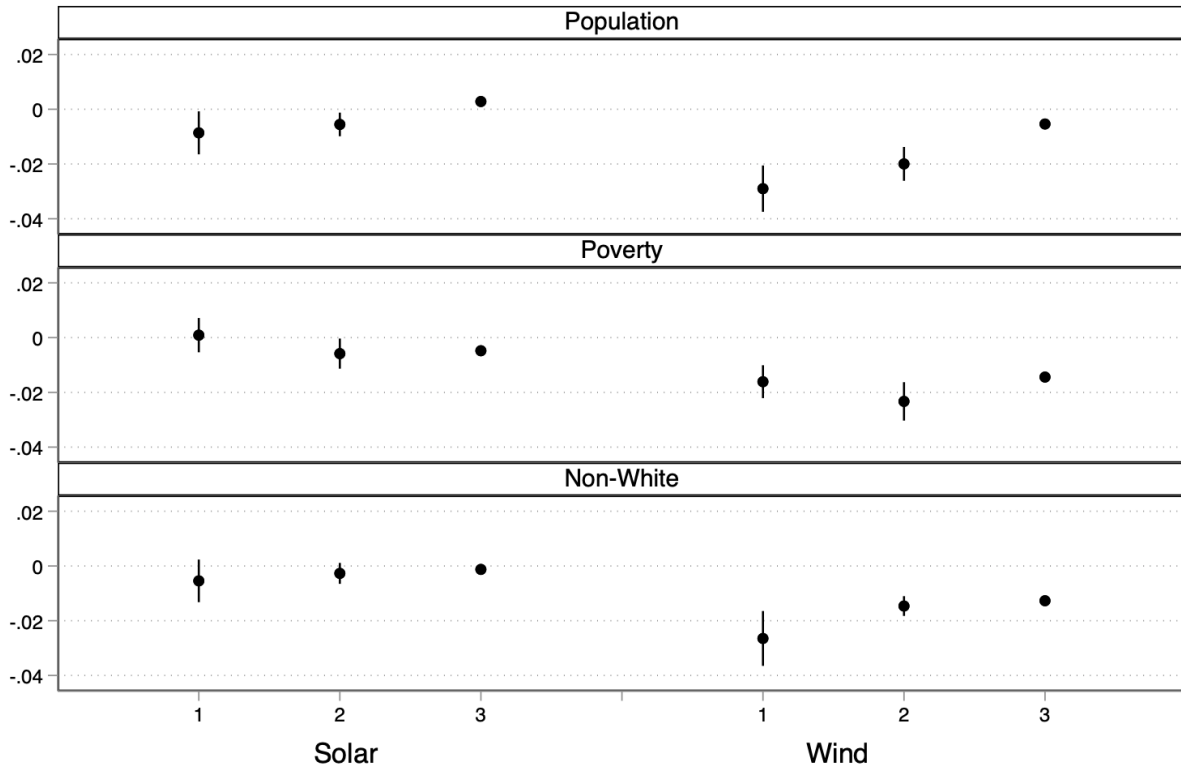


Figure 2: Effect of Solar and Wind on  $\text{NO}_x$  across Demographic Terciles

---

Notes: Coefficients represent change in hourly CAISO-wide lbs of  $\text{NO}_x$  emitted from natural gas generators per MWh of solar or wind generation, in each respective demographic tercile. All regressions include hour-by-month, month-by-year, and day-of-week fixed effects as well as linear controls for nuclear generation and quadratic controls for temperature, natural gas price, and hourly load for four regions in CAISO. Error bars constructed from standard errors clustered by week.

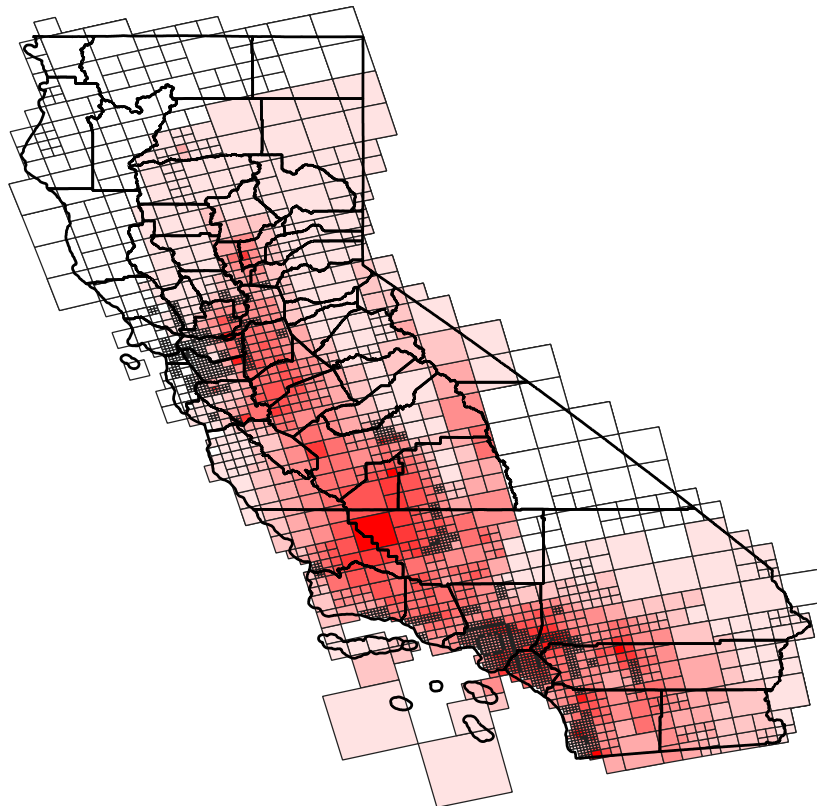


Figure 3: Change in PM 2.5 pollution due to renewables

Notes: Predicted changes in ground-level PM 2.5 from InMap due to renewables. Changes in emissions from natural gas plants due to renewables are based on empirical estimates in Table 6 (column 1). Darker grids indicate greater reductions in ground-level PM 2.5. Sources: InMap, Author calculations

Table 1: Summary Statistics of Hourly Grid Characteristics of CAISO

	Average	Average % Load
Total Hourly Load	25,798.85 MWh	
Natural Gas	8,287.336 MWh	(31%)
Wind	1,915 MWh	(7.6%)
Solar	3,326 MWh	(12.6%)
Imports	6,258.68 MWh	(24.6%)
Hydro	2,957.61 MWh	(11.5%)
NO <sub>x</sub> emissions	591.74 (lbs)	
<i>N</i>	14,973	

The sample includes 14,973 hourly observations of grid characteristics from April 2018 to December 2019. There are 25 missing observations due to a lack of solar data on September 22, 2018 and a missing hour of load data for one region of CAISO on October 31, 2018. The NO<sub>x</sub> emissions are calculated by multiplying a generator’s hourly heat input (if they generated electricity in that hour), by their corresponding emission rate.

Table 2: Summary Statistics of Demographic Terciles

	Average Population	Minimum	Maximum	# Generators	Total Capacity (GW)
1st Tercile	4,263	0	23,608	81	11.56
2nd Tercile	57,607	26,670	96,266	84	14.13
3rd Tercile	154,160	98,882	371,982	76	8.92
	Average Share Below Poverty Line	Minimum	Maximum	# Generators	Total Capacity (GW)
1st Tercile	0.08	0.03	0.12	82	13.82
2nd Tercile	0.17	0.13	0.21	85	11.99
3rd Tercile	0.27	0.23	0.38	71	7.96
	Average Share Non-White	Minimum	Maximum	# Generators	Total Capacity (GW)
1st Tercile	0.33	0.11	0.56	85	15.72
2nd Tercile	0.66	0.57	0.74	78	7.71
3rd Tercile	0.85	0.75	0.98	75	10.34

This sample includes 241 natural gas generators in CAISO. There are three generators (at a single plant) that have 0 people living within 3 miles and thus do not have any poverty/nonwhite data. This leaves 241 generators across the population bins, but 238 across the poverty/nonwhite bins. Terciles are not distributed evenly across terciles because there are multiple generators at a single plant.

Table 3: Aggregate CAISO responses to Solar and Wind

	(1) Natural Gas Generation	(2) Hydroelectric Generation	(3) Imports	(4) NO <sub>x</sub> Emissions
Solar	-0.376*** (0.0390)	-0.0339** (0.0130)	-0.434*** (0.0474)	-0.0111* (0.00565)
Wind	-0.598*** (0.0416)	-0.0455*** (0.0131)	-0.313*** (0.0352)	-0.0549*** (0.00730)
<i>N</i>	14,973	14,973	14,949	14,973
<i>R</i> <sup>2</sup>	0.934	0.921	0.844	0.694

Coefficients in columns 1-3 represent change in MWh of generation from natural gas, hydroelectric, and imports in CAISO per MWh of solar or wind generation. The dependent variable in Column 4 is aggregate NO<sub>x</sub> emissions. All regressions include hour-by-month, month-by-year, and day-of-week fixed effects. Load variables include quadratics of hourly load for four regions in CAISO. Quadratic controls for temperature and natural gas price are also included, along with linear controls for nuclear generation. Standard errors clustered by week included in parentheses.

\*  $p < 0.10$ , \*\*  $p < 0.05$ , \*\*\*  $p < 0.01$

Table 4: Alternative specifications (CAISO-wide results)

	Hourly Natural Gas Generation (MWh)				
	(1)	(2)	(3)	(4)	(5)
Solar	-0.635*** (0.0853)	-0.625*** (0.0847)	-0.379*** (0.0401)	-0.383*** (0.0403)	-0.376*** (0.0390)
Wind	-0.941*** (0.0909)	-0.946*** (0.0896)	-0.618*** (0.0404)	-0.608*** (0.0417)	-0.598*** (0.0416)
Nuclear		✓	✓	✓	✓
Load Variables			✓	✓	✓
Temperature				✓	✓
Natural Gas Price					✓
<i>N</i>	14,974	14,974	14,973	14,973	14,973
<i>R</i> <sup>2</sup>	0.787	0.789	0.932	0.933	0.934

Coefficients represent change in MWh of generation from natural gas generators in CAISO per MWh of solar or wind generation. All regressions include hour-by-month, month-by-year, and day-of-week fixed effects. We control as noted for hourly nuclear generation and include quadratic controls for temperature, nuclear generation, natural gas price, and hourly load for four regions in CAISO. Standard errors clustered by week included in parentheses.

\*  $p < 0.10$ , \*\*  $p < 0.05$ , \*\*\*  $p < 0.01$

Table 5: Effects of wind and solar across demographic terciles

		Natural Gas Generation (MWh)			NO <sub>x</sub> Emissions (lbs)		
		(1)	(2)	(3)	(4)	(5)	(6)
Population		1	2	3	1	2	3
	Solar	-0.223*** (0.0283)	-0.132*** (0.0160)	-0.0204** (0.00850)	-0.00862** (0.00395)	-0.00555** (0.00217)	0.00282 (0.00188)
	Wind	-0.328*** (0.0225)	-0.192*** (0.0212)	-0.0769*** (0.0110)	-0.0290*** (0.00426)	-0.0200*** (0.00311)	-0.00540*** (0.00174)
	<i>N</i>	14,973	14,973	14,973	14,973	14,973	14,973
	<i>R</i> <sup>2</sup>	0.913	0.875	0.852	0.586	0.568	0.345
Poverty share		1	2	3	1	2	3
	Solar	-0.0920*** (0.0128)	-0.135*** (0.0193)	-0.108*** (0.0135)	0.000893 (0.00315)	-0.00585** (0.00277)	-0.00479*** (0.00177)
	Wind	-0.177*** (0.0178)	-0.217*** (0.0201)	-0.173*** (0.0172)	-0.0161*** (0.00302)	-0.0233*** (0.00353)	-0.0144*** (0.00219)
	<i>N</i>	14,973	14,973	14,973	14,973	14,973	14,973
	<i>R</i> <sup>2</sup>	0.886	0.880	0.862	0.465	0.615	0.617
Share Non-white		1	2	3	1	2	3
	Solar	-0.0946*** (0.0136)	-0.107*** (0.0165)	-0.136*** (0.0161)	-0.00544 (0.00392)	-0.00270 (0.00192)	-0.00126 (0.00192)
	Wind	-0.186*** (0.0173)	-0.150*** (0.0162)	-0.226*** (0.0198)	-0.0265*** (0.00504)	-0.0146*** (0.00182)	-0.0127*** (0.00193)
	<i>N</i>	14,973	14,973	14,973	14,973	14,973	14,973
	<i>R</i> <sup>2</sup>	0.911	0.854	0.866	0.535	0.588	0.557

Coefficients represent change in aggregate MWh of generation or aggregate lbs NO<sub>x</sub> emitted from natural gas generators in each respective demographic tercile of plants in CAISO per MWh of solar or wind generation. All regressions include hour-by-month, month-by-year, and day-of-week fixed effects as well as linear controls for nuclear generation and quadratic controls for temperature, natural gas price, and hourly load for four regions in CAISO. Standard errors clustered by week included in parentheses.

\*  $p < 0.10$ , \*\*  $p < 0.05$ , \*\*\*  $p < 0.01$

Table 6: Interaction model with demographics

	Natural gas generation (MWh)			
	(1)	(2)	(3)	(4)
<b>Solar</b>				
Solar generation	-0.00363*** (0.000603)	-0.00210*** (0.000696)	-0.00263*** (0.000884)	-0.00250*** (0.000792)
$x$ Population	1.14e-08*** (3.56e-09)			1.12e-08*** (3.21e-09)
$x$ Poverty Share		-0.00295 (0.00331)		-0.00376 (0.00302)
$x$ Share Non-White			-0.00000113 (0.00135)	-0.000468 (0.00126)
<b>Wind</b>				
Wind generation	-0.00360*** (0.000541)	-0.00284** (0.00115)	-0.00298** (0.00119)	-0.00343*** (0.00129)
$x$ Population	1.72e-08*** (5.30e-09)			1.61e-08*** (5.37e-09)
$x$ Poverty Share		0.00323 (0.00609)		0.00129 (0.00519)
$x$ Share Non-White			0.00121 (0.00198)	-0.000436 (0.00177)
$N$	944,627	911,306	911,306	911,306
$R^2$	0.852	0.854	0.854	0.856

Coefficients represent change in MWh of natural gas generator's output per MWh increase in solar or wind generation. All regressions include generator, hour-by-month, month-by-year, and day-of-week fixed effects as well as linear controls for nuclear generation and quadratic controls for temperature, natural gas price, and hourly load for four regions in CAISO. Standard errors clustered by week and plant are included in parentheses. \*  $p < 0.10$ , \*\*  $p < 0.05$ , \*\*\*  $p < 0.01$

Table 7: Interaction effects with plant characteristics

	Natural gas generation (MWh)		
	(1)	(2)	(3)
Solar generation	-0.00231*** (0.000535)	-0.00205* (0.00111)	-0.00285*** (0.000511)
Wind generation	-0.00201*** (0.000442)	-0.00309* (0.00162)	-0.00250*** (0.000446)
Solar*SolarCap	-0.000000790** (0.000000307)		
Wind*WindCap	-0.000000809*** (0.000000282)		
Solar*HeatRate	-0.000134 (0.000173)		
Wind*HeatRate	0.000121 (0.000264)		
Solar*NBB	0.0000921 (0.000816)		
Wind*NBB	0.000572 (0.00124)		
<i>N</i>	944,627	944,627	944,627
<i>R</i> <sup>2</sup>	0.852	0.851	0.851

Interaction term coefficients represent heterogeneous responses in hourly MWh of generation of a natural gas generator per MWh of solar or wind generation. *SolarCap* and *WindCap* are the sum of solar or wind capacity within 75km of the natural gas generator. *HeatRate* is the generator's heat rate, and *NBB* is an indicator for whether the plant is a "non-backbone" plant that faces higher fuel costs. Regressions include hour-by-month, month-by-year, day-of-week, and generator fixed effects. Load variables include quadratics of hourly load for four regions in CAISO. Quadratic controls for weather-station level temperature, and natural gas price are included as well. Linear controls for nuclear generation included. Standard errors clustered by plant and by week included in parentheses.

\*  $p < 0.10$ , \*\*  $p < 0.05$ , \*\*\*  $p < 0.01$

Table 8: Plant location and plant characteristics

Population Terciles				
Solar Terciles	1	2	3	Total
1	23	42	17	82
2	21	23	35	79
3	37	19	24	80
Wind Terciles	1	2	3	Total
1	17	35	33	85
2	44	22	18	84
3	20	27	25	72
Heat Rate Terciles	1	2	3	Total
1	27	24	30	81
2	33	29	18	80
3	21	31	28	80
NBB	1	2	3	Total
0	66	62	69	197
1	15	22	7	44
Total	81	84	76	241

Distribution of the 241 natural gas generators across population terciles (based of number of individuals living within a 3 mile radius) and a. solar and wind capacity terciles (based on the amount of solar and wind capacity within 75 km), b. heat rate terciles and c. indicator for non-backbone generator.

Table 9: Effects of solar and wind on congestion prices by population tercile

	Population Terciles		
	(1)	(2)	(3)
<b>Full Sample</b>			
Solar generation	0.000153 (0.000177)	-0.0000599 (0.0000876)	-0.000170 (0.000163)
Wind generation	-0.000597*** (0.000166)	-0.000279*** (0.0000978)	-0.000262 (0.000200)
N	650012	731768	760783
$R^2$	0.049	0.027	0.079
	Population Terciles		
	(1)	(2)	(3)
<b>Trim MCC Outliers</b>			
Solar generation	-0.000153*** (0.0000409)	-0.0001000** (0.0000439)	-0.000142* (0.0000798)
Wind generation	-0.0000914** (0.0000444)	-0.0000403 (0.0000494)	-0.000106 (0.0000874)
N	635698	718581	741636
$R^2$	0.054	0.057	0.133
	Population Terciles		
	(1)	(2)	(3)
<b>Trim MCC Outliers, Limit to Daytime Hours</b>			
Solar generation	-0.000186*** (0.0000470)	-0.0000877 (0.0000589)	-0.0000754 (0.0000991)
Wind generation	-0.000154** (0.0000591)	-0.0000786 (0.0000759)	-0.0000878 (0.000132)
N	286709	325916	334681
$R^2$	0.069	0.070	0.149

Coefficients represent change in nodal marginal congestion cost (MCC) per MWh increase in solar or wind generation. Trim specifications drop 1% outliers on either side of the MCC distribution (-30and56). Daytime hours 8am-6pm. All regressions include hour-by-month, month-by-year, day-of-week, and nodal fixed effects as well as quadratic controls for temperature, natural gas price, and hourly load for four regions in CAISO. Linear controls for nuclear generation included. Standard errors clustered by week and county are included in parentheses. \*  $p < 0.10$ , \*\*  $p < 0.05$ , \*\*\*  $p < 0.01$

Table 10: Annual Avoided Emissions and Damages

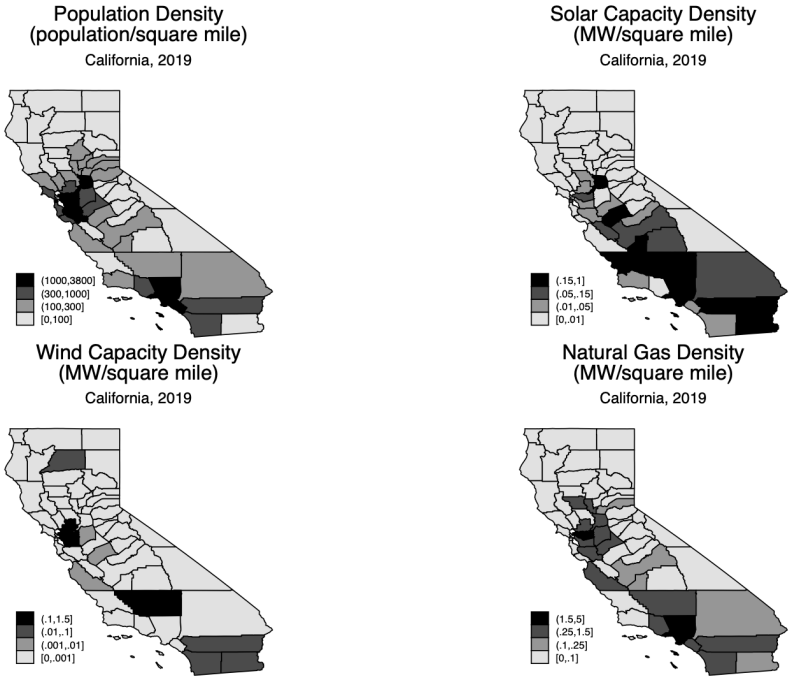
	<b>NO<sub>x</sub></b>		<b>PM2.5</b>	
	Avoided Emissions	Avoided Damages	Avoided Emissions	Avoided Damages
<b>1st Population Tercile</b>				
Solar	123 tons	\$1,166,354	96 tons	\$8,287,683
Wind	231 tons	\$2,185,028	79 tons	\$6,787,944
Total	354 tons	\$3,351,382	175 tons	\$15,075,626
<b>2nd Population Tercile</b>				
Solar	79 tons	\$1,318,229	57 tons	\$10,407,053
Wind	159 tons	\$2,645,234	46 tons	\$8,429,294
Total	238 tons	\$3,963,463	103 tons	\$18,836,347
<b>3rd Population Tercile</b>				
Solar	0	0	9 tons	\$2,015,829
Wind	40 tons	\$740,444	18 tons	\$4,231,417
Total	40 tons	\$740,444	27 tons	\$6,247,246

Tercile-specific avoided emissions are calculated using the hourly solar and wind generation in 2019 multiplied by the tercile-specific coefficients for decreases in NO<sub>x</sub> or natural gas generation (used for approximate decreases in PM2.5). The tercile-specific damages multiply the tercile's avoided emissions by the tercile-specific damage per ton.

Online Appendix for  
The distributional benefits of emission reductions from renewable energy

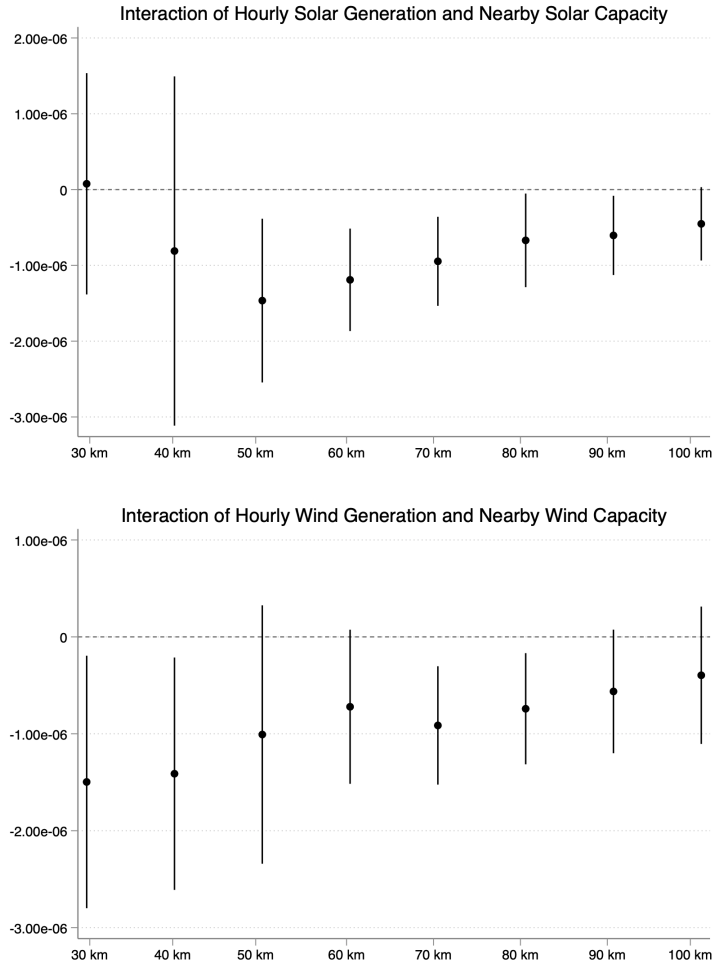
# A Appendix Figures and Tables

Figure A.1: County level capacity and population in California



Sources: EIA, Census

Figure A.2: Effect of renewable capacity on generation response - alternative distance bins



Coefficients represent change in hourly MWh of generation from natural gas generators interacted with cumulative wind or solar capacity within a given distance band. All regressions include hour-by-month, month-by-year, and day-of-week fixed effects as well as quadratic controls for temperature, natural gas price, and hourly load for four regions in CAISO. Linear controls for nuclear generation included. Standard errors clustered by plant and week represented by error bars.

Figure A.3: Scatter plot between Population and Renewable Capacity

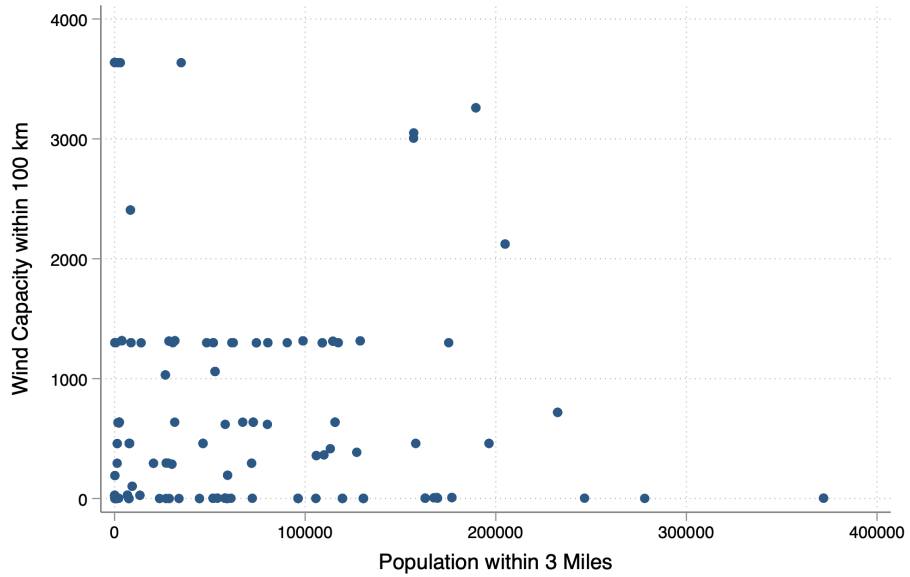
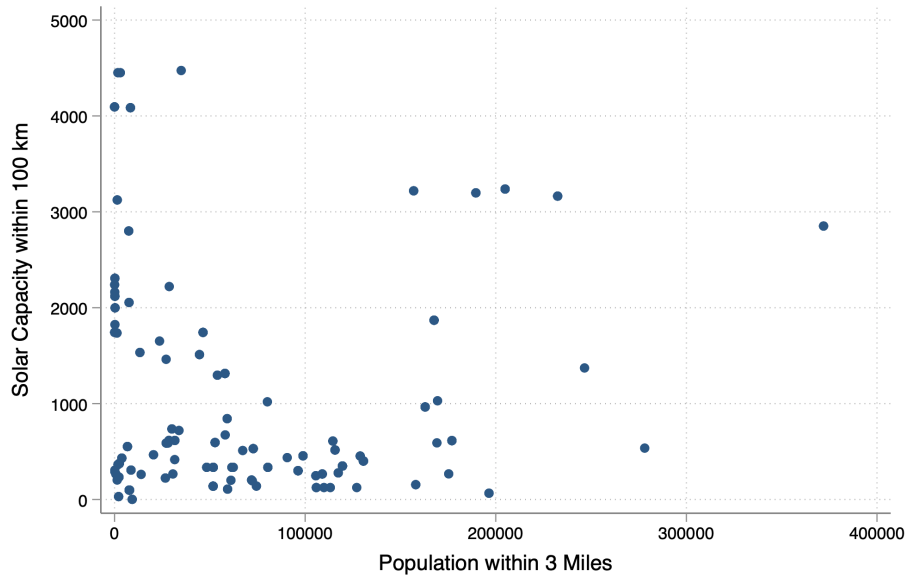


Figure A.4: Scatter plot between Population and Heat Rates

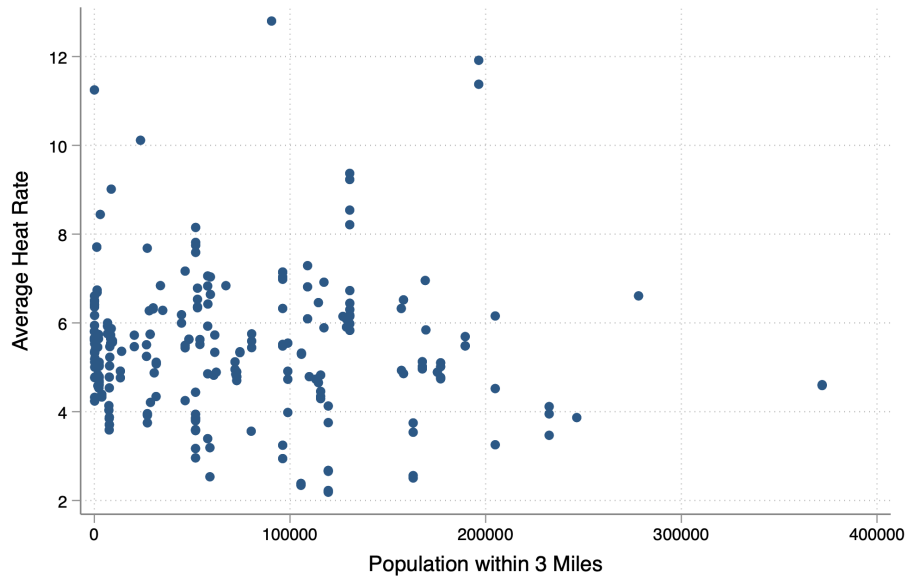
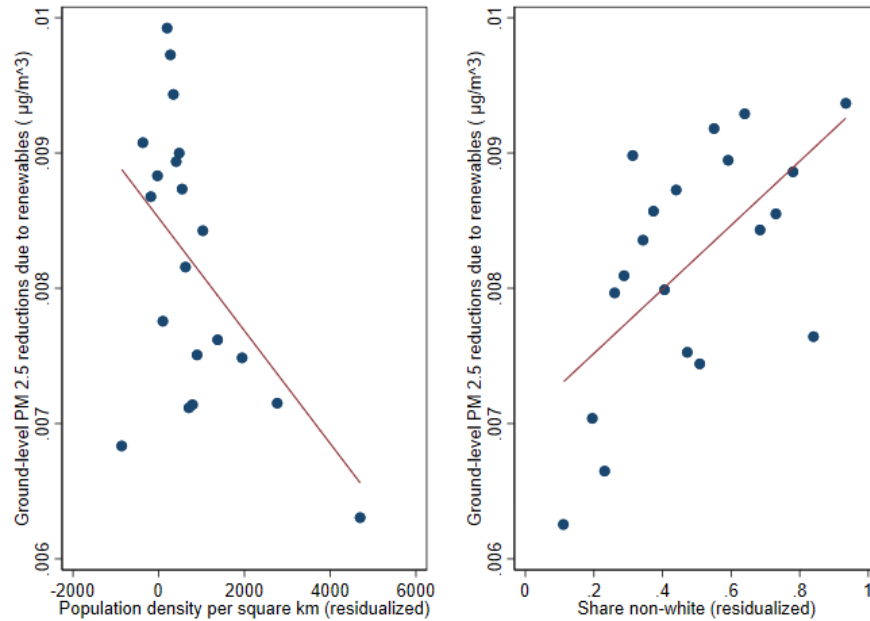
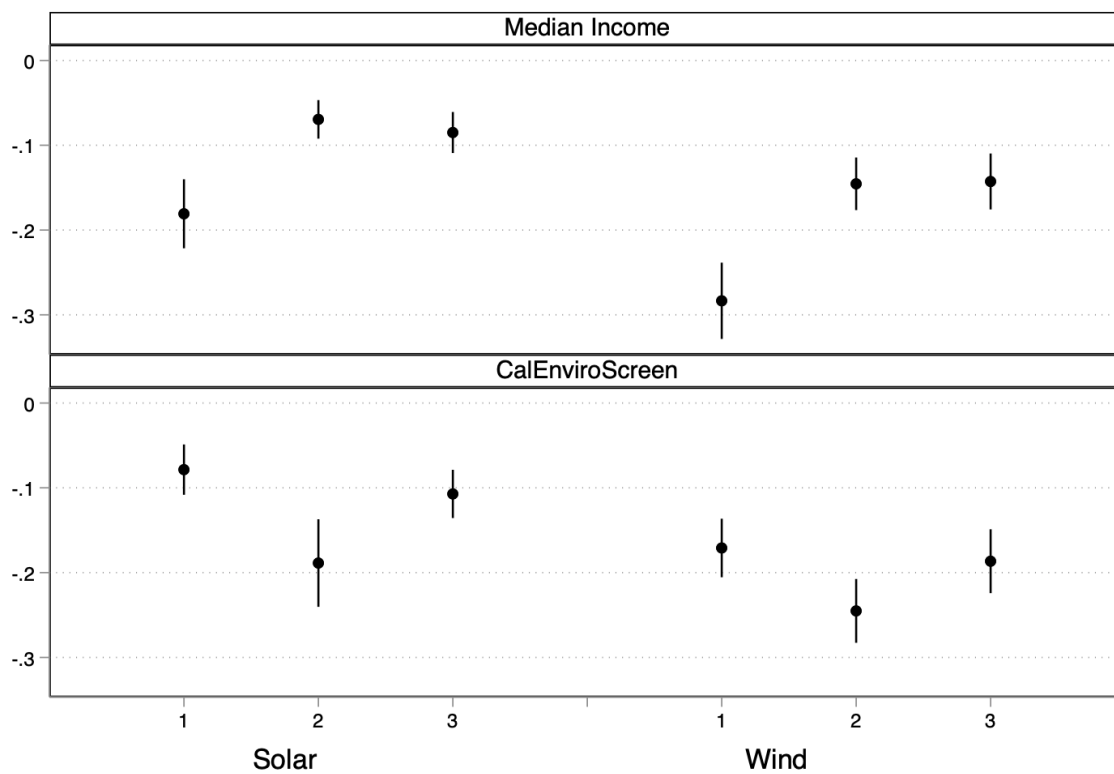


Figure A.5: InMap predicted PM 2.5 reductions and demographics



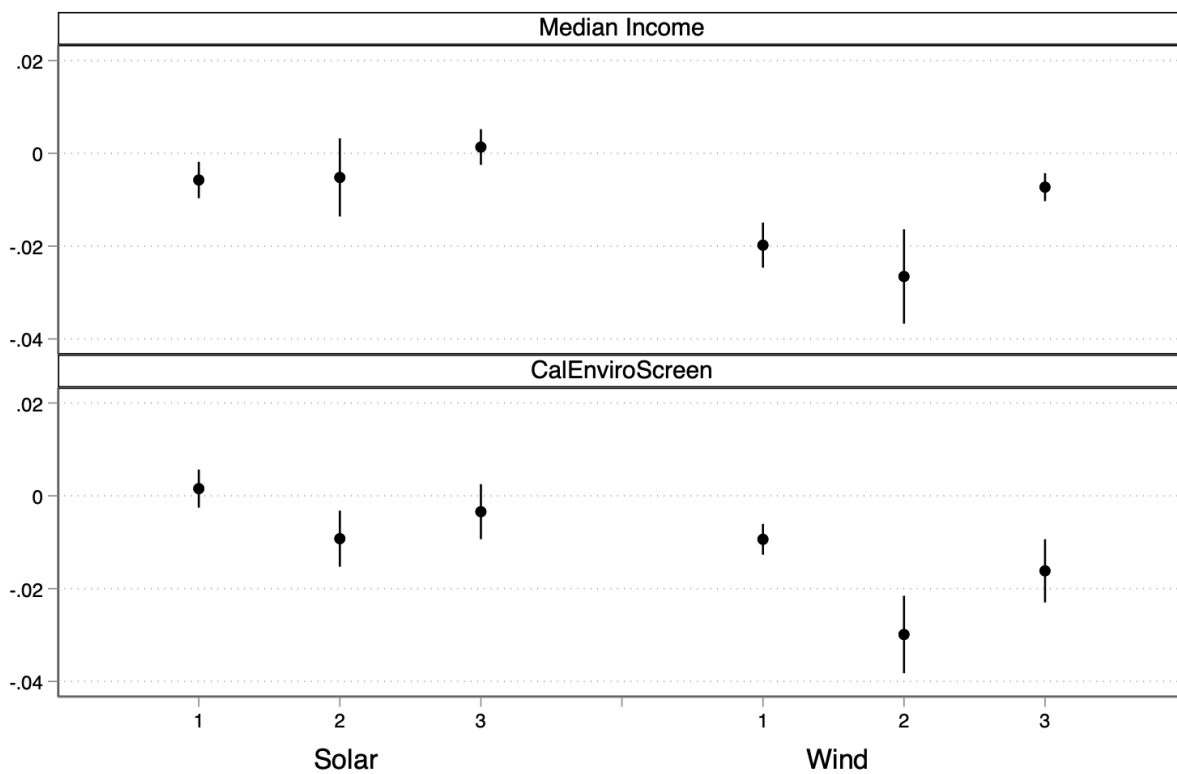
Binscatter plot of InMap predicted ground-level PM 2.5 reductions due to renewables versus population density and share non-white. Baseline PM 2.5 is controlled for and corresponds to InMap's baseline prediction of PM 2.5 levels. Share non-white and Population density are calculated per InMap grid. Emission reductions that enter the InMap model are based on population interaction model (Table 6).

Figure A.6: Effect of Solar and Wind on Natural Gas Generation across Demographic Terciles - alternative metrics



Coefficients represent change in hourly MWh of generation from natural gas generators in each respective demographic tercile of plants in CAISO per MWh of solar or wind generation. All regressions include hour-by-month, month-by-year, and day-of-week fixed effects as well as quadratic controls for temperature, natural gas price, and hourly load for four regions in CAISO. Linear controls for nuclear generation included. Standard errors clustered by week included in parentheses.

Figure A.7: Effect of Solar and Wind on  $\text{NO}_x$  across Demographic Terciles - alternative metrics



Coefficients represent change in hourly lbs of  $\text{NO}_x$  emitted from natural gas generators in each respective demographic tercile of plants in CAISO per MWh of solar or wind generation. All regressions include hour-by-month, month-by-year, and day-of-week fixed effects as well as quadratic controls for temperature, natural gas price, and hourly load for four regions in CAISO. Linear controls for nuclear generation included. Standard errors clustered by week included in parentheses.

Figure A.8: Population Results across Utilities

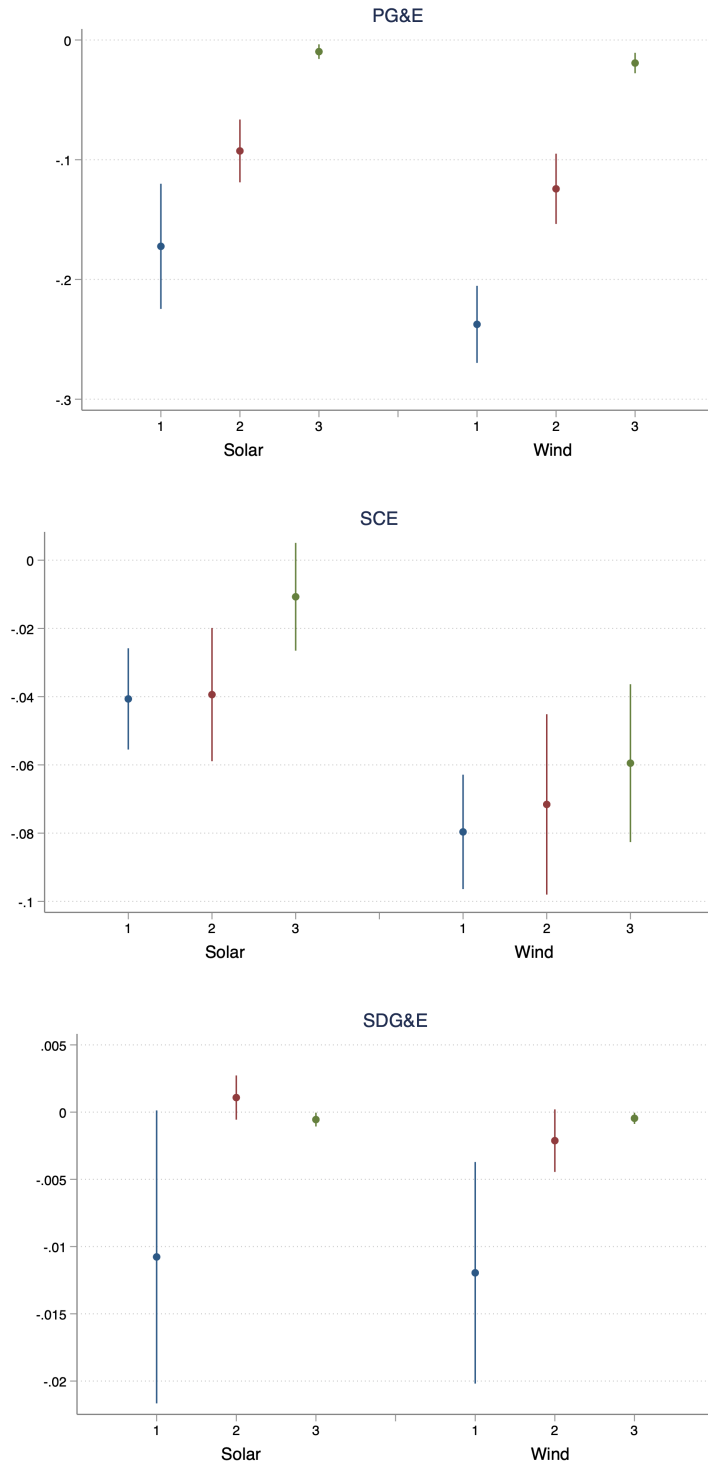


Figure A.9: Poverty Line Results across Utilities

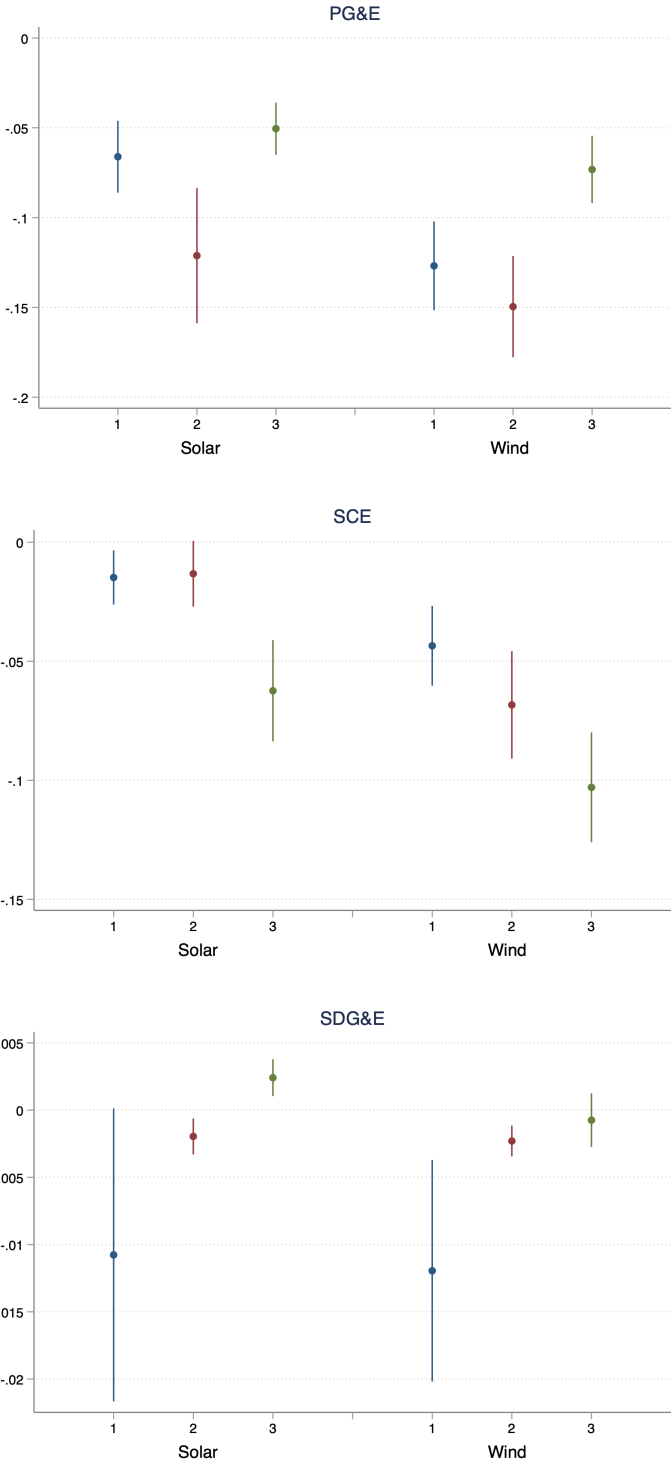


Figure A.10: Median Income Results across Utilities

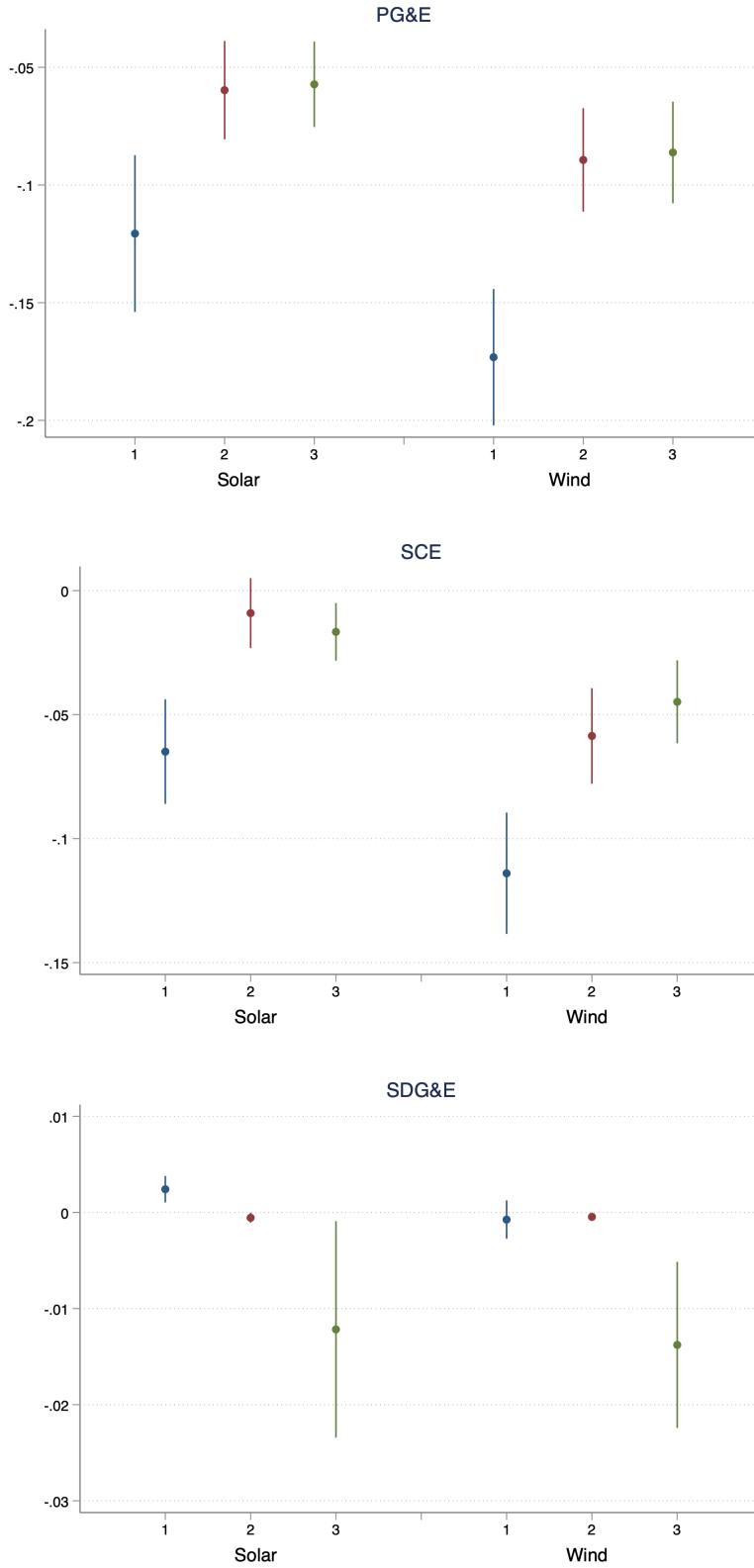


Figure A.11: Share Minority Results across Utilities

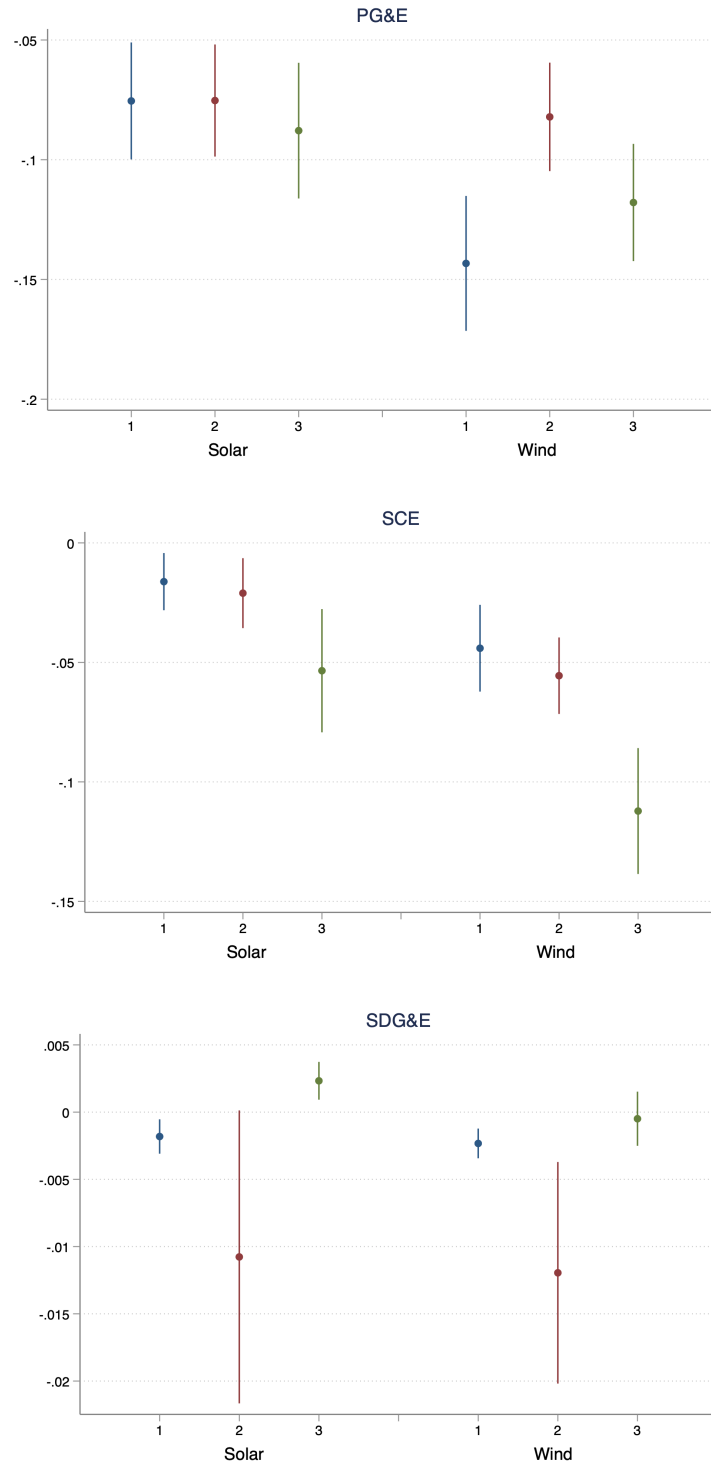
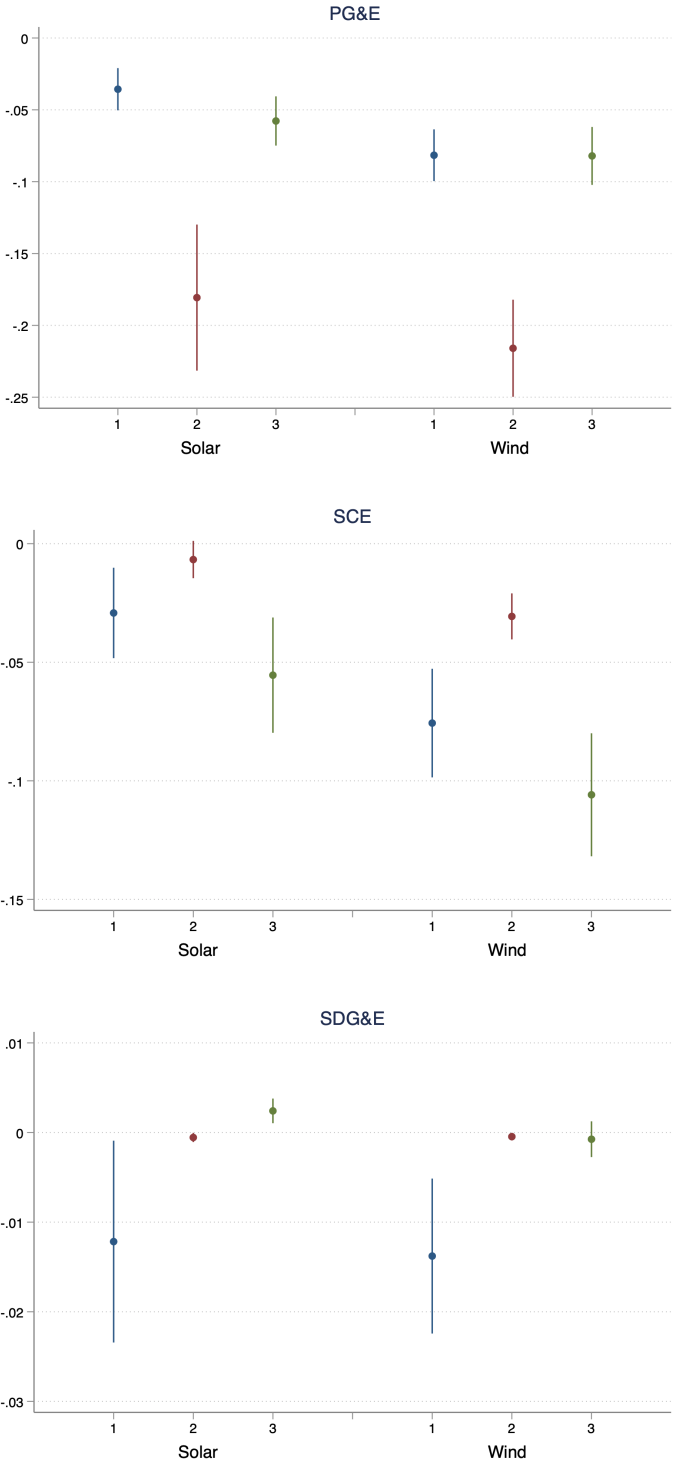


Figure A.12: CalEnviroScreen Results across Utilities



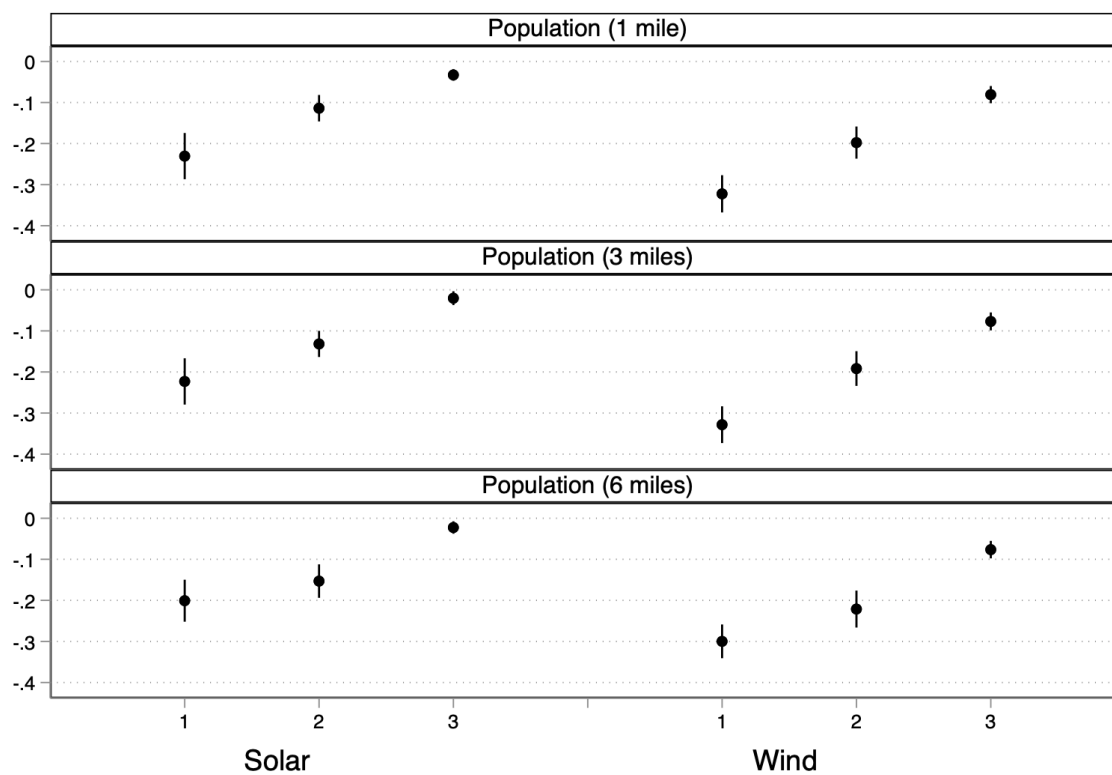


Figure A.13: Effect of Solar and Wind on Natural Gas Generation across Population Terciles - alternative demographic radii

Notes: Coefficients represent change in hourly CAISO-wide MWh generation from natural gas generators per MWh of solar or wind generation, in each respective population tercile. All regressions include hour-by-month, month-by-year, and day-of-week fixed effects as well as linear controls for nuclear generation and quadratic controls for temperature, natural gas price, and hourly load for four regions in CAISO. Error bars constructed from standard errors clustered by week.

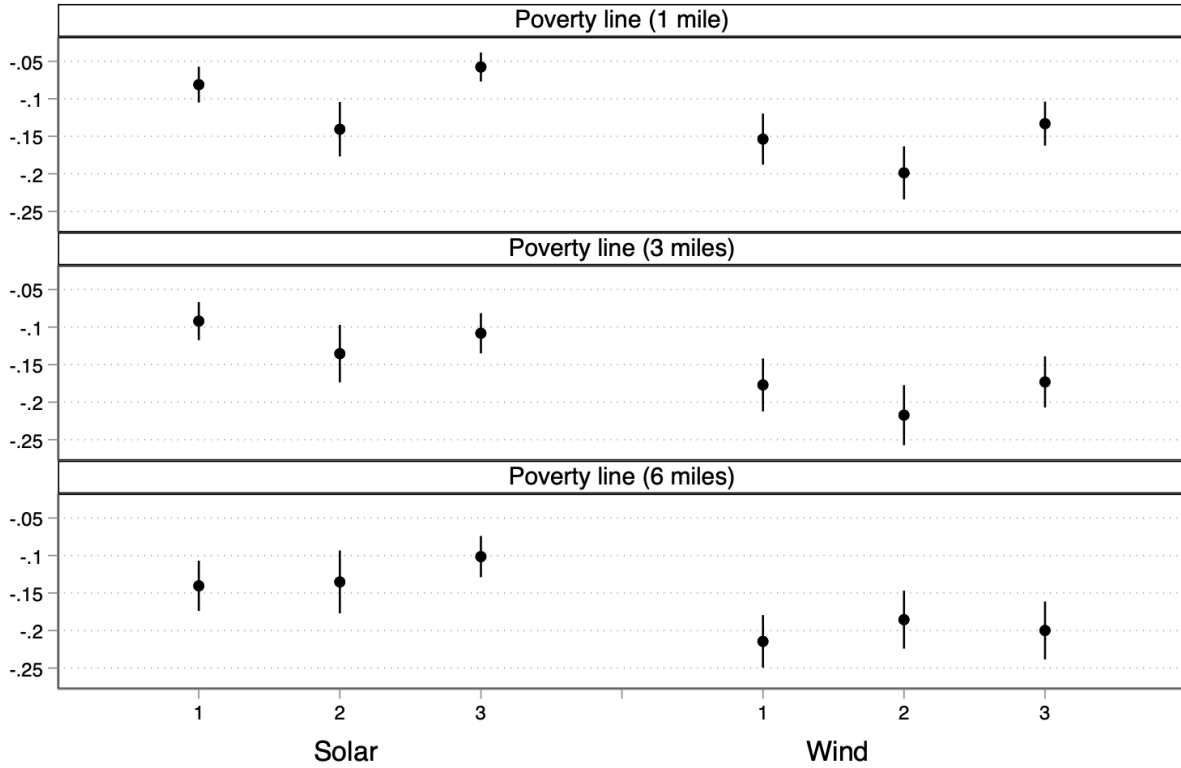


Figure A.14: Effect of Solar and Wind on Natural Gas Generation across Share below Poverty Line Terciles - alternative demographic radii

Notes: Coefficients represent change in hourly CAISO-wide MWh generation from natural gas generators per MWh of solar or wind generation, in each respective share below poverty line tercile. All regressions include hour-by-month, month-by-year, and day-of-week fixed effects as well as linear controls for nuclear generation and quadratic controls for temperature, natural gas price, and hourly load for four regions in CAISO. Error bars constructed from standard errors clustered by week.

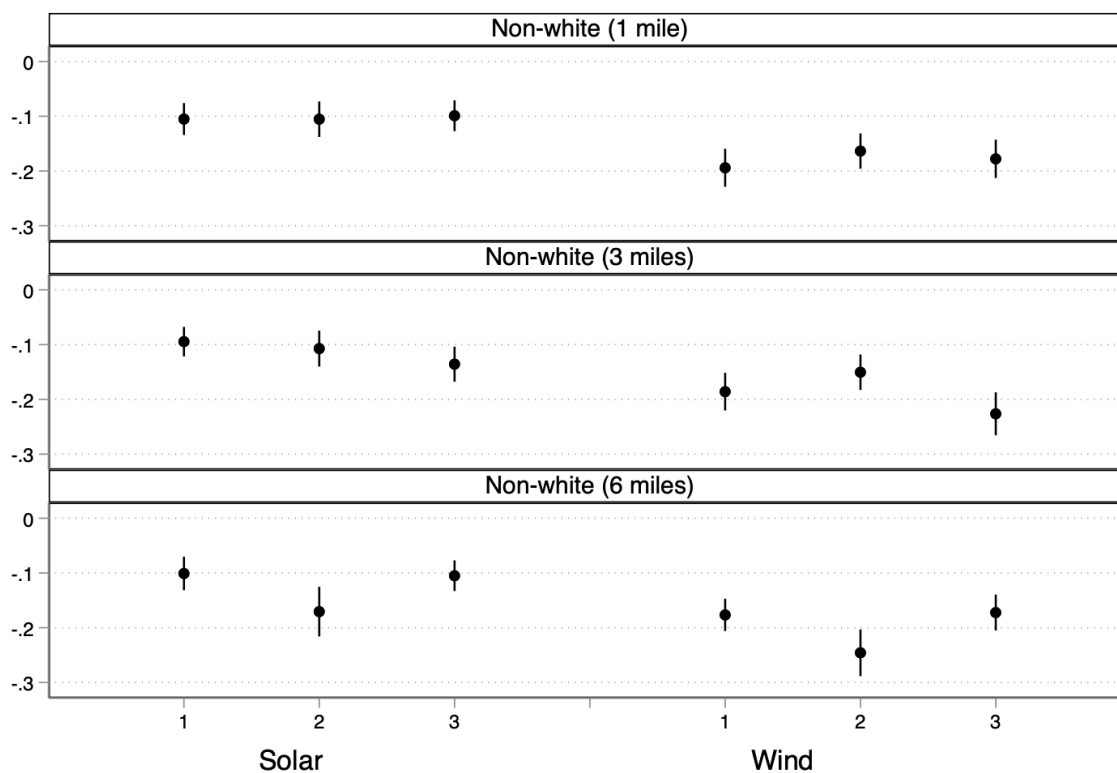


Figure A.15: Effect of Solar and Wind on Natural Gas Generation across Share Nonwhite Terciles - alternative demographic radii

Notes: Coefficients represent change in hourly CAISO-wide MWh generation from natural gas generators per MWh of solar or wind generation, in each respective share nonwhite tercile. All regressions include hour-by-month, month-by-year, and day-of-week fixed effects as well as linear controls for nuclear generation and quadratic controls for temperature, natural gas price, and hourly load for four regions in CAISO. Error bars constructed from standard errors clustered by week.

Table A.1: Solar and wind omitted variable bias

	CAISO hourly load			
	(1)	(2)	(3)	(4)
Solar	0.339 *** (0.0381)	0.255 *** (0.0313)	-0.319 *** (0.0806)	-0.284 *** (0.0741)
Wind	0.302 ** (0.123)	-0.0261 (0.0924)	-0.408 *** (0.0871)	-0.226 *** (0.0600)
Nuclear	1.803 *** (0.387)	0.156 (0.280)	0.223 (0.288)	-0.0168 (0.189)
Day of week FE	✓	✓	✓	✓
Year by month FE		✓	✓	✓
Month by hour FE			✓	✓
Temperature controls				✓
<i>N</i>	14,974	14,974	14,974	14,974
<i>R</i> <sup>2</sup>	0.151	0.474	0.860	0.893

Coefficients represent change in MWh of hourly load in CAISO per MWh of solar, wind, or nuclear generation. All regressions include day-of-week fixed effects. Hour-by-month and month-by-year fixed effects are included where noted. Temperature controls include a quadratic for hourly temperature. Linear controls for nuclear generation included. Standard errors clustered by week included in parentheses. \*  $p < 0.10$ , \*\*  $p < 0.05$ , \*\*\*  $p < 0.01$

Table A.2: Alternative specifications - Generators in 1st Pop Tercile

Hourly Natural Gas Generation (MWh)					
From Generators in 1st Population Tercile					
	(1)	(2)	(3)	(4)	(5)
Solar	-0.316*** (0.0402)	-0.310*** (0.0400)	-0.222*** (0.0281)	-0.221*** (0.0285)	-0.223*** (0.0283)
Wind	-0.450*** (0.0393)	-0.452*** (0.0387)	-0.329*** (0.0223)	-0.330*** (0.0225)	-0.328*** (0.0225)
Nuclear		✓	✓	✓	✓
Load Variables			✓	✓	✓
Temperature				✓	✓
Natural Gas Price					✓
<i>N</i>	14,974	14,974	14,973	14,973	14,973
<i>R</i> <sup>2</sup>	0.830	0.833	0.912	0.912	0.913

Coefficients represent change in MWh of generation from natural gas generators in lowest population tercile of plants in CAISO per MWh of solar or wind generation. All regressions include hour-by-month, month-by-year, and day-of-week fixed effects as well as quadratic controls for temperature, natural gas price, and hourly load for four regions in CAISO. Linear controls for nuclear generation included. Standard errors clustered by week included in parentheses. \*  $p < 0.10$ , \*\*  $p < 0.05$ , \*\*\*  $p < 0.01$

Table A.3: Effect of Solar and Wind on gas generation (Generator-level estimates)

Natural Gas Generation	
Solar	-0.00283*** (0.000322)
Wind	-0.00238*** (0.000233)
<i>N</i>	944,627
<i>R</i> <sup>2</sup>	0.851

Coefficients represent the average change in MWh of generation from a natural gas generator in CAISO per MWh of solar or wind generation. Regression include hour-by-month, month-by-year, day-of-week, and generator fixed effects. Load variables include quadratics of hourly load for four regions in CAISO. Linear controls for nuclear generation included. Quadratic controls for weather-station level temperature and natural gas price are included as well. Standard errors clustered by week included in parentheses.

\*  $p < 0.10$ , \*\*  $p < 0.05$ , \*\*\*  $p < 0.01$

Table A.4: Ground-level PM2.5 reductions due to renewables (InMap)

	PM 2.5 reductions			
	(1) Level	(2) Log	(3) Level	(4) Log
Baseline PM 2.5	0.00200*** (8.37e-05)	0.241*** (0.0112)	0.00128*** (4.88e-05)	0.214*** (0.00996)
Share non-white	0.00352*** (0.000494)	0.603*** (0.0695)	0.00278*** (0.000354)	0.629*** (0.0652)
Population density (persons per km <sup>2</sup> )	-6.29e-07*** (9.31e-08)	-5.39e-05*** (1.22e-05)	-6.22e-07*** (5.93e-08)	-0.000103*** (1.14e-05)
Interactions	Population	Population	All	All
InMap grids	2,657	2,374	2,657	2,297
$R^2$	0.435	0.367	0.399	0.347

Coefficients represent the level or percent change in PM 2.5 reductions due to renewables per InMap grid as predicted by InMap modeling. There are 2,657 grids in California with non-zero population. Baseline PM 2.5 is InMap's baseline prediction of PM 2.5 levels. Share non-white and Population density are calculated per InMap grid. Columns (1) and (2) use predicted emission reductions based on population interactions (Table 6) which then enter the InMap model, while columns (3) and (4) use predicted emission reductions based on all interactions (population, share non-white, and share below poverty line). Robust standard errors included in parentheses.

\*  $p < 0.10$ , \*\*  $p < 0.05$ , \*\*\*  $p < 0.01$

Table A.5: Summary statistics of demographic terciles

	Average Median Income	Minimum	Maximum	# Generators	Total Capacity (GW)
1st Tercile	\$41,491	\$18,109	\$51,019	80	10.8
2nd Tercile	\$61,231	\$51,093	\$73,449	79	10.2
3rd Tercile	\$95,834	\$73,865	\$131,246	79	12.6
	Average CalEnviroScreen	Minimum	Maximum	# Generators	Total Capacity (GW)
1st Tercile	30	7	46	88	14.1
2nd Tercile	63	48	74	76	11.8
3rd Tercile	85	75	99	79	8.6

This sample includes 241 natural gas generators in CAISO. There are three generators (at a single plant) that have 0 people living within 3 miles. Therefore they do not have any income data. This leaves 241 generators across the population bins, but 238 across median income terciles. Terciles are not distributed evenly because there are multiple generators at a single plant. The CalEnviroScreen is equal to the product of each component, geographic and socioeconomic (which each take a value 1-10), such that CalEnviroScreen ranges between 1-100.

Table A.6: Coefficient estimates – median Income & CalEnviroScreen

	Natural Gas Generation (MWh)			NO <sub>x</sub> Emissions (lbs)		
	(1)	(2)	(3)	(4)	(5)	(6)
Median Income						
	1	2	3	1	2	3
Solar	-0.181*** (0.0205)	-0.0695*** (0.0114)	-0.0850*** (0.0122)	-0.00575*** (0.00197)	-0.00520 (0.00424)	0.00135 (0.00194)
Wind	-0.283*** (0.0226)	-0.145*** (0.0156)	-0.143*** (0.0166)	-0.0198*** (0.00244)	-0.0265*** (0.00512)	-0.00729*** (0.00152)
<i>N</i>	14,973	14,973	14,973	14,973	14,973	14,973
<i>R</i> <sup>2</sup>	0.899	0.864	0.872	0.653	0.553	0.331
CalEnviroScreen						
	1	2	3	1	2	3
Solar	-0.0785*** (0.0149)	-0.189*** (0.0260)	-0.107*** (0.0143)	0.00156 (0.00206)	-0.00923*** (0.00304)	-0.00341 (0.00298)
Wind	-0.171*** (0.0174)	-0.245*** (0.0189)	-0.187*** (0.0190)	-0.00936*** (0.00167)	-0.0299*** (0.00420)	-0.0162*** (0.00343)
<i>N</i>	14,973	14,973	14,973	14,973	14,973	14,973
<i>R</i> <sup>2</sup>	0.883	0.895	0.850	0.367	0.639	0.528

Coefficients represent change in aggregate MWh of generation or aggregate lbs NO<sub>x</sub> emitted from natural gas generators in each respective demographic tercile of plants in CAISO per MWh of solar or wind generation. All regressions include hour-by-month, month-by-year, and day-of-week fixed effects as well as quadratic controls for temperature, natural gas price, and hourly load for four regions in CAISO. Linear controls for nuclear generation included. Standard errors clustered by week included in parentheses.

\*  $p < 0.10$ , \*\*  $p < 0.05$ , \*\*\*  $p < 0.01$

Table A.7: Population and socioeconomic terciles

Median Income Terciles	Population Terciles			
	1	2	3	Total
1	47	21	12	80
2	14	24	41	79
3	17	39	23	79
Poverty Line Terciles	1	2	3	Total
1	26	37	19	82
2	18	29	38	85
3	34	18	19	71
Total	78	84	76	238

This shows the distribution of the 241 natural gas generators across population, median income, and poverty rate terciles (based on number of individuals, median income and % living under poverty line within a 3 mile radius).

Table A.8: Demographic correlations

<b>Entire Sample</b>					
	Population	CalEnviroScreen	Median Income	Share Below Poverty Line	Share Non-White
Population	1				
CalEnviroScreen	0.180	1			
Median Income	0.130	-0.436	1		
Share Below Poverty Line	-0.00519	0.379	-0.741	1	
Share Non-White	0.209	0.410	-0.0952	0.159	1
<b>PG&amp;E</b>					
	Population	CalEnviroScreen	Median Income	Share Below Poverty Line	Share Non-White
Population	1				
CalEnviroScreen	-0.136	1			
Median Income	0.257	-0.521	1		
Share Below Poverty Line	0.0289	0.589	-0.697	1	
Share Non-White	0.209	0.353	0.0432	0.0996	1
<b>SCE</b>					
	Population	CalEnviroScreen	Median Income	Share Below Poverty Line	Share Non-White
Population	1				
CalEnviroScreen	0.501	1			
Median Income	0.277	-0.223	1		
Share Below Poverty Line	-0.178	0.0933	-0.771	1	
Share Non-White	0.366	0.621	-0.437	0.332	1
<b>SDG&amp;E</b>					
	Population	CalEnviroScreen	Median Income	Share Below Poverty Line	Share Non-White
Population	1				
CalEnviroScreen	-0.291	1			
Median Income	-0.239	-0.851	1		
Share Below Poverty Line	0.259	0.826	-0.959	1	
Share Non-White	-0.768	0.526	-0.108	0.0265	1

Table A.9: Interaction model including zero generation values

	Natural Gas Generation (MWh)			
	(1)	(2)	(3)	(4)
Solar generation	-0.00215*** (0.000494)	-0.000897** (0.000394)	-0.00117* (0.000676)	-0.00125** (0.000590)
Solar * Population	7.88e-09*** (2.94e-09)			6.92e-09** (2.77e-09)
Solar * Poverty Line		-0.00329 (0.00219)		-0.00288 (0.00227)
Solar * Non-white			-0.000467 (0.00108)	-0.000343 (0.00109)
Wind	-0.00456*** (0.00105)	-0.000650 (0.00162)	-0.00290 (0.00308)	-0.00298 (0.00287)
Wind * Population	2.83e-08** (1.11e-08)			2.66e-08** (1.08e-08)
Wind * Poverty Line		-0.0108 (0.00976)		-0.0131 (0.00968)
Wind * Non-white			0.000695 (0.00495)	0.00139 (0.00477)
<i>N</i>	3541774	3496876	3496876	3496876
<i>R</i> <sup>2</sup>	0.554	0.546	0.546	0.548

Standard errors in parentheses

\*  $p < 0.10$ , \*\*  $p < 0.05$ , \*\*\*  $p < 0.01$

Coefficients represent the change in hourly MWh of generation of a natural gas generator per MWh of solar or wind generation. Regressions include hour-by-month, month-by-year, day-of-week, and generator fixed effects. Load variables include quadratics of hourly load for four regions in CAISO. Quadratic controls for weather-station level temperature, and natural gas price are included as well. Linear controls for nuclear generation included. Standard errors clustered by plant and by week included in parentheses.

\*  $p < 0.10$ , \*\*  $p < 0.05$ , \*\*\*  $p < 0.01$

Table A.10: Interaction Model with Median Income & CalEnviroScreen

	Natural Gas Generation (MWh)			
	Median Income		CalEnviroScreen	
	Single (1)	Joint (2)	Single (3)	Joint (4)
Solar generation	-0.00375*** (0.000951)	-0.00413*** (0.00116)	-0.00222** (0.000845)	-0.00239*** (0.000868)
Solar $x$ Median Income	1.77e-08 (1.17e-08)	1.60e-08 (1.04e-08)		
Solar $x$ CalEnviroScreen			-0.0000101 (0.0000116)	-0.0000161 (0.0000114)
Solar $x$ Population		1.07e-08*** (3.09e-09)		1.17e-08*** (3.33e-09)
Solar $x$ Share Non-white		-0.000486 (0.00119)		-0.000208 (0.00130)
Wind Generation	-0.00278** (0.00132)	-0.00397** (0.00171)	-0.00359** (0.00137)	-0.00372*** (0.00137)
Wind $x$ Median Income	8.07e-09 (1.93e-08)	8.73e-09 (1.78e-08)		
Wind $x$ CalEnviroScreen		0.0000200 (0.0000213)		0.0000131 (0.0000196)
Wind $x$ Population		1.60e-08*** (5.24e-09)		1.56e-08*** (5.26e-09)
Wind $x$ Share Non-white		-0.0000396 (0.00185)		-0.000829 (0.00181)
$N$	911306	911306	944627	911306
$R^2$	0.855	0.856	0.851	0.856

Coefficients represent the change in hourly MWh of generation of a natural gas generator per MWh of solar or wind generation. Regressions include hour-by-month, month-by-year, day-of-week, and generator fixed effects. Load variables include quadratics of hourly load for four regions in CAISO. Quadratic controls for weather-station level temperature, and natural gas price are included as well. Linear controls for nuclear generation included. Standard errors clustered by plant and by week included in parentheses.

\*  $p < 0.10$ , \*\*  $p < 0.05$ , \*\*\*  $p < 0.01$

Table A.11: Hourly Load & Natural Gas Generation by Utility

	PG&E	SCE	SDG&E
Load	11,574 MWh	11,761 MWh	2,270 MWh
Natural Gas Generation	5,481 MWh	2,560 MWh	209 MWh

These averages are based on hourly data from CAISO from April 2018 to December 2019.

Table A.12: Population tercile estimates across utilities

	Natural Gas Generation (MWh)			NO <sub>x</sub> Emissions (lbs)		
	(1)	(2)	(3)	(4)	(5)	(6)
	Population Terciles			Population Terciles		
<b>PG&amp;E</b>	1	2	3	1	2	3
Solar	-0.172*** (0.0263)	-0.0926*** (0.0132)	-0.00971*** (0.00307)	-0.00476*** (0.00107)	-0.00285** (0.00120)	-0.000435** (0.000166)
Wind	-0.237*** (0.0162)	-0.124*** (0.0148)	-0.0192*** (0.00430)	-0.0122*** (0.00119)	-0.00774*** (0.000935)	-0.00102*** (0.000234)
<i>N</i>	14,973	14,973	14,972	14,973	14,973	14,972
<i>R</i> <sup>2</sup>	0.903	0.840	0.719	0.687	0.559	0.528
<b>SCE</b>						
Solar	-0.0407*** (0.00747)	-0.0394*** (0.00982)	-0.0107 (0.00795)	-0.00364 (0.00325)	-0.00303* (0.00161)	0.00330* (0.00190)
Wind	-0.0796*** (0.00844)	-0.0716*** (0.0133)	-0.0595*** (0.0116)	-0.0167*** (0.00374)	-0.0127*** (0.00255)	-0.00442** (0.00175)
<i>N</i>	14,973	14,973	14,973	14,973	14,973	14,973
<i>R</i> <sup>2</sup>	0.722	0.755	0.819	0.428	0.408	0.307
<b>SDG&amp;E</b>						
Solar	-0.0108* (0.00548)	0.00108 (0.000827)	-0.000554** (0.000259)	0.000708 (0.00130)	0.000150 (0.000381)	-0.0000635* (0.0000353)
Wind	-0.0119*** (0.00415)	-0.00212* (0.00117)	-0.000460** (0.000211)	-0.000485 (0.000320)	0.000122 (0.000507)	-0.0000725** (0.0000325)
<i>N</i>	14,973	14,973	14,973	14,973	14,973	14,973
<i>R</i> <sup>2</sup>	0.446	0.796	0.354	0.048	0.239	0.182

Coefficients represent change in aggregate MWh of generation or aggregate lbs NO<sub>x</sub> emitted from natural gas generators in each respective demographic tercile of plants in each of the three utilities per MWh of solar or wind generation. All regressions include hour-by-month, month-by-year, and day-of-week fixed effects as well as quadratic controls for temperature, natural gas price, and hourly load for four regions in CAISO. Linear controls for nuclear generation included. Standard errors clustered by week included in parentheses. \*  $p < 0.10$ , \*\*  $p < 0.05$ , \*\*\*  $p < 0.01$

Table A.13: Poverty share estimates across utilities

	Natural Gas Generation (MWh)			NO <sub>x</sub> Emissions (lbs)		
	(1)	(2)	(3)	(4)	(5)	(6)
	Poverty Terciles			Poverty Terciles		
<b>PG&amp;E</b>	1	2	3	1	2	3
Solar	-0.0661*** (0.0101)	-0.121*** (0.0189)	-0.0505*** (0.00733)	-0.000287 (0.000550)	-0.00470*** (0.00131)	-0.00190*** (0.000435)
Wind	-0.127*** (0.0124)	-0.150*** (0.0142)	-0.0732*** (0.00942)	-0.00615*** (0.000564)	-0.00946*** (0.00131)	-0.00435*** (0.000589)
<i>N</i>	14,973	14,973	14,973	14,973	14,973	14,973
<i>R</i> <sup>2</sup>	0.852	0.860	0.829	0.566	0.569	0.699
<b>SCE</b>						
Solar	-0.0148** (0.00573)	-0.0133* (0.00695)	-0.0624*** (0.0107)	0.000680 (0.00268)	-0.000912 (0.00235)	-0.00297* (0.00150)
Wind	-0.0435*** (0.00843)	-0.0683*** (0.0114)	-0.103*** (0.0116)	-0.00990*** (0.00289)	-0.0134*** (0.00278)	-0.0107*** (0.00173)
<i>N</i>	14,973	14,973	14,973	14,973	14,973	14,973
<i>R</i> <sup>2</sup>	0.837	0.772	0.749	0.385	0.476	0.475
<b>SDG&amp;E</b>						
Solar	-0.0108* (0.00548)	-0.00196*** (0.000674)	0.00241*** (0.000692)	0.000708 (0.00130)	-0.000231** (0.0000892)	0.000332 (0.000383)
Wind	-0.0119*** (0.00415)	-0.00230*** (0.000576)	-0.000747 (0.00100)	-0.000485 (0.000320)	-0.000367*** (0.0000775)	0.000305 (0.000488)
<i>N</i>	14,973	14,973	14,966	14,973	14,973	14,966
<i>R</i> <sup>2</sup>	0.446	0.384	0.868	0.048	0.196	0.237

Coefficients represent change in aggregate MWh of generation or aggregate lbs NO<sub>x</sub> emitted from natural gas generators in each respective demographic tercile of plants in each of the three utilities per MWh of solar or wind generation. All regressions include hour-by-month, month-by-year, and day-of-week fixed effects as well as quadratic controls for temperature, natural gas price, and hourly load for four regions in CAISO. Linear controls for nuclear generation included. Standard errors clustered by week included in parentheses. \*  $p < 0.10$ , \*\*  $p < 0.05$ , \*\*\*  $p < 0.01$

Table A.14: Median income estimates across utilities

	Natural Gas Generation (MWh)			NO <sub>x</sub> Emissions (lbs)		
	(1)	(2)	(3)	(4)	(5)	(6)
	Median Income Terciles			Median Income Terciles		
<b>PG&amp;E</b>	1	2	3	1	2	3
Solar	-0.121*** (0.0168)	-0.0597*** (0.0105)	-0.0572*** (0.00913)	-0.00346*** (0.000799)	-0.00244** (0.00113)	-0.000822 (0.000533)
Wind	-0.173*** (0.0146)	-0.0893*** (0.0111)	-0.0862*** (0.0109)	-0.00924*** (0.00110)	-0.00629*** (0.000873)	-0.00452*** (0.000556)
<i>N</i>	14,973	14,973	14,973	14,973	14,973	14,973
<i>R</i> <sup>2</sup>	0.880	0.857	0.793	0.616	0.522	0.534
<b>SCE</b>						
Solar	-0.0649*** (0.0106)	-0.00907 (0.00709)	-0.0166*** (0.00586)	-0.00233 (0.00151)	-0.00267 (0.00390)	0.00167 (0.00136)
Wind	-0.114*** (0.0123)	-0.0586*** (0.00970)	-0.0449*** (0.00843)	-0.0115*** (0.00174)	-0.0198*** (0.00466)	-0.00237 (0.00147)
<i>N</i>	14,973	14,973	14,973	14,973	14,973	14,973
<i>R</i> <sup>2</sup>	0.765	0.738	0.842	0.484	0.476	0.217
<b>SDG&amp;E</b>						
Solar	0.00241*** (0.000692)	-0.000554** (0.000259)	-0.0122** (0.00567)	0.000332 (0.000383)	-0.0000635* (0.0000353)	0.000541 (0.00132)
Wind	-0.000747 (0.00100)	-0.000460** (0.000211)	-0.0138*** (0.00435)	0.000305 (0.000488)	-0.0000725** (0.0000325)	-0.000779** (0.000348)
<i>N</i>	14,966	14,973	14,973	14,966	14,973	14,973
<i>R</i> <sup>2</sup>	0.868	0.354	0.458	0.237	0.182	0.060

Coefficients represent change in aggregate MWh of generation or aggregate lbs NO<sub>x</sub> emitted from natural gas generators in each respective demographic tercile of plants in each of the three utilities per MWh of solar or wind generation. All regressions include hour-by-month, month-by-year, and day-of-week fixed effects as well as quadratic controls for temperature, natural gas price, and hourly load for four regions in CAISO. Linear controls for nuclear generation included. Standard errors clustered by week included in parentheses. \*  $p < 0.10$ , \*\*  $p < 0.05$ , \*\*\*  $p < 0.01$

Table A.15: Share non-white Results across Utilities

	Natural Gas Generation (MWh)			NO <sub>x</sub> Emissions (lbs)		
	(1)	(2)	(3)	(4)	(5)	(6)
	Share non-white Terciles			Share non-white Terciles		
<b>PG&amp;E</b>	1	2	3	1	2	3
Solar	-0.0754*** (0.0123)	-0.0753*** (0.0118)	-0.0878*** (0.0143)	-0.00229** (0.00107)	-0.00167** (0.000669)	-0.00293*** (0.000786)
Wind	-0.143*** (0.0142)	-0.0821*** (0.0114)	-0.118*** (0.0123)	-0.00745*** (0.000884)	-0.00499*** (0.000630)	-0.00740*** (0.00105)
<i>N</i>	14,973	14,973	14,973	14,973	14,973	14,973
<i>R</i> <sup>2</sup>	0.879	0.824	0.818	0.517	0.652	0.540
<b>SCE</b>						
Solar	-0.0162*** (0.00602)	-0.0210*** (0.00736)	-0.0535*** (0.0130)	-0.00305 (0.00360)	-0.00142 (0.00125)	0.00111 (0.00169)
Wind	-0.0441*** (0.00913)	-0.0556*** (0.00805)	-0.112*** (0.0133)	-0.0181*** (0.00459)	-0.00919*** (0.00165)	-0.00644*** (0.00131)
<i>N</i>	14,973	14,973	14,973	14,973	14,973	14,973
<i>R</i> <sup>2</sup>	0.846	0.760	0.766	0.461	0.486	0.353
<b>SDG&amp;E</b>						
Solar	-0.00181*** (0.000644)	-0.0108* (0.00548)	0.00233*** (0.000707)	-0.000196** (0.0000853)	0.000708 (0.00130)	0.000291 (0.000390)
Wind	-0.00233*** (0.000556)	-0.0119*** (0.00415)	-0.000492 (0.00101)	-0.000371*** (0.0000739)	-0.000485 (0.000320)	0.000387 (0.000493)
<i>N</i>	14,973	14,973	14,973	14,973	14,973	14,973
<i>R</i> <sup>2</sup>	0.385	0.446	0.865	0.194	0.048	0.239

Coefficients represent change in aggregate MWh of generation or aggregate lbs NO<sub>x</sub> emitted from natural gas generators in each respective demographic tercile of plants in each of the three utilities per MWh of solar or wind generation. All regressions include hour-by-month, month-by-year, and day-of-week fixed effects as well as quadratic controls for temperature, natural gas price, and hourly load for four regions in CAISO. Linear controls for nuclear generation included. Standard errors clustered by week included in parentheses. \*  $p < 0.10$ , \*\*  $p < 0.05$ , \*\*\*  $p < 0.01$

Table A.16: CalEnviroScreen Results across Utilities

	Natural Gas Generation (MWh)			NO <sub>x</sub> Emissions (lbs)		
	(1)	(2)	(3)	(4)	(5)	(6)
	CalEnviroScreen Terciles			CalEnviroScreen Terciles		
<b>PG&amp;E</b>	1	2	3	1	2	3
Solar	-0.0356*** (0.00739)	-0.181*** (0.0256)	-0.0578*** (0.00862)	-0.000145 (0.000363)	-0.00484*** (0.00135)	-0.00286*** (0.000651)
Wind	-0.0816*** (0.00906)	-0.216*** (0.0170)	-0.0821*** (0.0101)	-0.00382*** (0.000403)	-0.0119*** (0.00110)	-0.00549*** (0.000927)
<i>N</i>	14,973	14,973	14,973	14,973	14,973	14,973
<i>R</i> <sup>2</sup>	0.855	0.882	0.817	0.596	0.670	0.509
<b>SCE</b>						
Solar	-0.0292*** (0.00960)	-0.00669* (0.00396)	-0.0554*** (0.0122)	0.00127 (0.00138)	-0.00416 (0.00253)	-0.000461 (0.00270)
Wind	-0.0756***	-0.0307***	-0.106***	-0.00497***	-0.0174***	-0.0121***
<i>N</i>	14,973	14,973	14,973	14,973	14,973	14,973
<i>R</i> <sup>2</sup>	0.848	0.770	0.749	0.290	0.476	0.409
<b>SDG&amp;E</b>						
Solar	-0.0122** (0.00567)	-0.000554** (0.000259)	0.00241*** (0.000692)	0.000541 (0.00132)	-0.0000635* (0.0000353)	0.000332 (0.000383)
Wind	-0.0138*** (0.00435)	-0.000460** (0.000211)	-0.000747 (0.00100)	-0.000779** (0.000348)	-0.0000725** (0.0000325)	0.000305 (0.000488)
<i>N</i>	14,973	14,973	14,966	14,973	14,973	14,966
<i>R</i> <sup>2</sup>	0.458	0.354	0.868	0.060	0.182	0.237

Coefficients represent change in aggregate MWh of generation or aggregate lbs NO<sub>x</sub> emitted from natural gas generators in each respective demographic tercile of plants in each of the three utilities per MWh of solar or wind generation. All regressions include hour-by-month, month-by-year, and day-of-week fixed effects as well as quadratic controls for temperature, natural gas price, and hourly load for four regions in CAISO. Linear controls for nuclear generation included. Standard errors clustered by week included in parentheses. \*  $p < 0.10$ , \*\*  $p < 0.05$ , \*\*\*  $p < 0.01$

Table A.17: Emissions Damages per ton by population tercile

Population Tercile	NO <sub>x</sub> damages (\$/ton)	PM2.5 damages (\$/ton)
1	\$9,457	\$86,590
2	\$16,602	\$183,693
3	\$18,589	\$230,231
California County Average	\$14,684	\$160,971

These tercile-specific damages are a capacity-weighted average of the damages per ton for the corresponding counties the generators are located in. The California average is the overall average of county damages across the state.

Table A.18: Results in Hours with Low versus High Renewable Share

	Low Renewable Share (<20%)			High Renewable Share (>20%)		
	Natural Gas Generation (MWh)					
Population Tercile	(1)	(2)	(3)	(1)	(2)	(3)
Solar	-0.186*** (0.0406)	-0.0937*** (0.0277)	0.00627 (0.0171)	-0.231*** (0.0262)	-0.139*** (0.0171)	-0.0266*** (0.00971)
Wind	-0.359*** (0.0224)	-0.213*** (0.0258)	-0.0651*** (0.0129)	-0.297*** (0.0259)	-0.173*** (0.0188)	-0.0896*** (0.0126)
$N$	8,968	8,968	8,968	5,961	5,961	5,961
$R^2$	0.902	0.846	0.809	0.923	0.913	0.895
	NO <sub>x</sub> Emissions (lbs)					
Population Tercile	(1)	(2)	(3)	(1)	(2)	(3)
Solar	-0.0118 (0.00943)	0.00760 (0.00882)	0.00766** (0.00336)	-0.00390 (0.00516)	-0.00613** (0.00272)	0.00311 (0.00213)
Wind	-0.0356*** (0.00518)	-0.0231*** (0.00437)	-0.00465*** (0.00127)	-0.0199*** (0.00482)	-0.0185*** (0.00314)	-0.00570* (0.00289)
$N$	8,968	8,968	8,968	5,961	5,961	5,961
$R^2$	0.601	0.527	0.314	0.587	0.626	0.366

Coefficients represent change in aggregate MWh of generation or aggregate lbs NO<sub>x</sub> emitted from natural gas generators in each respective demographic tercile of plants in each of the three utilities per MWh of solar or wind generation. All regressions include hour-by-month, month-by-year, and day-of-week fixed effects as well as quadratic controls for temperature, natural gas price, and hourly load for four regions in CAISO. Linear controls for nuclear generation included. Standard errors clustered by week included in parentheses. \*  $p < 0.10$ , \*\*  $p < 0.05$ , \*\*\*  $p < 0.01$

Table A.19: Price effect interacted with population

	Congestion cost (\$/MWh)
	(1)
Solar generation	-0.000170*** (0.0000574)
$x$ Population	1.05e-09** (4.60e-10)
Wind generation	-0.000153 (0.0000995)
$x$ Population	4.99e-11 (8.51e-10)
$N$	947306
$R^2$	0.092

Coefficients represent change in marginal congestion cost of a node (\$/MWh) per MWh increase in solar or wind generation. All regressions include hour-by-month, month-by-year, day-of-week, and nodal fixed effects as well as linear controls for nuclear generation and quadratic controls for temperature, natural gas price, and hourly load for four regions in CAISO. Observations are limited to daytime hours and 1% outliers on either side are dropped. Standard errors clustered by week and county are included in parentheses. \*  $p < 0.10$ , \*\*  $p < 0.05$ , \*\*\*  $p < 0.01$